NBER WORKING PAPER SERIES

THE WORK-AT-HOME TECHNOLOGY BOON AND ITS CONSEQUENCES

Morris A. Davis
Andra C. Ghent
Jesse M. Gregory

Working Paper 28461
http://www.nber.org/papers/w28461

NATIONAL BUREAU OF ECONOMIC RESEARCH
1050 Massachusetts Avenue
Cambridge, MA 02138
February 2021

We thank Tim Landvoigt, Andrii Parkhomenko, and Stijn Van Nieuwerburgh for helpful comments on an earlier draft. The views expressed herein are those of the authors and do not necessarily reflect the views of the National Bureau of Economic Research.

The Work-at-Home Technology Boon and its Consequences
Morris A. Davis, Andra C. Ghent, and Jesse M. Gregory
NBER Working Paper No. 28461
February 2021
JEL No. O33,O41,R12,R33

ABSTRACT

We study the impact of widespread adoption of work-at-home technology using an equilibrium model where people choose where to live, how to allocate their time between working at home and at the office, and how much space to use in production. A key parameter is the elasticity of substitution between working at home and in the office that we estimate using cross-sectional time-use data. The model indicates that the pandemic induced a large change to the relative productivity of working at home which will permanently affect incomes, income inequality, and city structure.

Morris A. Davis
Rutgers University
Rutgers Business School
Newark, NJ 07102
mdavis@business.rutgers.edu

Andra C. Ghent
Department of Finance
Kenan-Flager Business School
University of North Carolina at Chapel Hill
300 Kenan Center Drive
Chapel Hill, NC 27599
andra_ghent@kenan-flagler.unc.edu

Jesse M. Gregory
Department of Economics
University of Wisconsin, Madison
1180 Observatory Drive
Madison, WI 53706-1393
and NBER
jmgregory@ssc.wisc.edu

1 Introduction

The work-at-home revolution has been slowly brewing for more than 30 years. The oldest of us (Davis) can recall distinct technological advances that have contributed to our ability to work effectively at home. In the early 1990s, affordable PCs running Microsoft Word and Excel became widely available. In the mid 1990s, work email became pervasive and the Netscape IPO lead a rush to explore the possibilities of the World Wide Web. In the early 2000s, high-speed-internet became widely available and by 2010 cellphones turned to smartphones. Finally, between 2010 and 2020 video-conferencing technology became useable and cloud-computing became cheap and convenient, facilitating remote meetings and data sharing across the world.

A common theme of each of these innovations is that their impact on the ability to do work depends at least in part, on the prevalence of adoption. There is no point to writing an email if no one reads it, video-conferencing becomes very difficult if the person on the receiving end has slow internet, and so forth. While many home-office technologies have been around for a while, the technologies become much more useful after widespread adoption.

We study the impact of the COVID-19 pandemic on the change in the productivity of working at home and document how this change will affect our incomes, where and how we work, where we live, and the demand and price of office space and housing. We postulate that the pandemic accelerated the widespread adoption of technologies that enable households to produce market work at home which, in turn, permanently raised the relative productivity of working at home.

To understand the consequences of this change in home productivity, we specify a model where high-skill workers can freely allocate their time to working at home or in the office. There is no commute to working at home and the productivity of working at home differs from that at the office. High-skill workers also choose how much physical space to rent at home and in the office. All workers choose where to live, how much to consume, and how much housing to rent.

A key parameter in the model is the elasticity of substitution between market work done at home and market work done in the office. With a high elasticity, small changes in technology can lead to a large shift in behavior. For example, imagine that working at home and in the office are perfect substitutes. This can lead to "bang-bang" behavior, where little time is spent working at home up to a certain level of work-at-home technology, after which a lot of time is spent working at home. Thus, our understanding of how changes to work-at-home technology will affect outcomes is intimately related to the elasticity of substitution in production between work done at home and work in the office.

We use the model to estimate this elasticity of substitution from a cross-section of data on high-skill workers from the American Time Use Survey (ATUS). In particular, the 2017-2018 Leave and Job Flexibility (LJF) module includes information on the frequency of work from home. Given an elasticity of substitution, the model predicts an exact relationship between the time spent commuting (which is a function of location choice) and the time households spend working at home vs. at the office. As the price of working in the office (commuting time) rises, people should spend more time working at home, and at a rate that depends on the elasticity of substitution. We use a GMM procedure to correct for measurement error in the commute-time data to bracket the elasticity of substitution between working at home and working at the office between 3 and 7.

After parameterizing the model, we simulate the model to understand the impact of the pandemic on work-at-home technology and its implications. We first study a "before" period, call it 2019, where high-skill workers work at home 20% of the time.

Given the model structure, this pins down the level of work-at-home technology prior to the onset of the pandemic. We then study an “after” period, call it 2022, where high-skill workers double their time working at home, which is the lower bound on estimates of the post-COVID increase in work-from-home. This expected doubling in hours worked at home sizes the gain in work-at-home productivity that occurred during the pandemic. Finally, we then study the pandemic period itself – a period in which we cut office productivity by 50%, reflecting the impact of social distancing on productivity at the office.

Our key result is that the widespread adoption of work-at-home technology increased the productivity of working at home relative to the productivity of working in the office by 34% between the onset and the end of the pandemic. The higher productivity of work from home leads to an approximately 20% decline in office rents in the central business district (CBD) in the short-run and long-run if the supply of office space cannot be reduced relative to pre-pandemic levels. Residential rents rise in the short-run, especially in the outer suburbs, due to increased demand for home office space. Hours worked at home increases even more in the long-run after the supply of space in residential areas has a chance to adjust. Since only high-skill workers can work at home in our model, the large gains to the technology from working at home increases income inequality between low- and high-skill workers. Finally, there is a small decline in productivity in the CBD due to a decrease in agglomeration economies.

We also simulate what would have happened if the COVID pandemic had occurred in 1990, prior to the existence of many work-at-home technologies. We assume that, in 1989, relative home productivity is 1/3 its 2019 value and that it does not change after the onset of the pandemic in 1990. As with the 2020 pandemic, we characterize the 1990 pandemic by a 50% drop in relative productivity in working at the office.

During this hypothetical 1990 pandemic, people continue to work at the office at the same rate and do not substitute into working at home. Incomes and prices fall, but there is no increased demand to work at home in the suburbs. According to our model, in 1990 working at home is not a practical alternative to working in the office.

As this 1990 counterfactual simulation indicates, the long-term effects of the COVID depend critically on work-from-home technology being available but not yet fully adopted. Overall, our model suggests the COVID pandemic will lead to higher income lifetime for the working population because it forced many households to work at home which boosted work-at-home productivity. While the measured gains to productivity we report of working at home likely would have happened eventually, the pandemic accelerated the process.

The findings of the paper have implications for municipal finance and environmental sustainability. The model suggests high-skill workers will increasingly relocate to more distant suburbs and CBD office rents (and therefore prices and property taxes) will fall, suggesting the budgets of central cities will be strained. While workers commuting less will reduce their carbon footprints, to the extent that home offices are less energy efficient than offices in large, well-built buildings, the net effect on sustainability is unclear.

Our paper relates to four distinct literatures. The first is how technological innovations get adopted and diffuse. Comin and Mestieri (2014) discuss the diffusion process in detail and several drivers of the pace of technological adoption. We find that COVID radically accelerated the use of work-from-home technology due to a large positive externality in adoption. Katz and Shapiro (1986) and Brock and Durlauf (2010) theoretically study technology adoption in the presence of network externalities more specifically. Our finding of a positive externality in technology adoption in work-from-home technology is also consistent with what Foster and Rosenzweig (2010) posit for health innovations.

The second literature we speak to is the effect of technological adoption on household lifestyles. Greenwood, Seshadri, and Yorukoglu (2005) argue that the consumer durable goods revolution, borne out of electricity, liberated women from the drudgery of home production. A related literature discusses how this home production technology influences the use of time spent working at the office and working on home production over the business cycle; see, for example, McGrattan, Rogerson, and Wright (1997).

A more recent literature studies work-from-home specifically. Bloom, Liang, Roberts, and Ying (2014) and Emanuel and Harrington (2020) find that call center workers are more productive when working from home. We study a broader class of workers whose work is less routine on average such that work from home may be less productive. Our focus, however, is on the substitutability between work-at-home and office work. Understanding this substitutability is important for understanding the long-term implications of changes to work-at-home technology. Our findings also demonstrate how the COVID shock could make us permanently more productive in aggregate. Instead of studying the productivity of working from home, Mas and Pallais (2017) study how workers value it and find that prospective call centers employees are willing to take an 8% cut in pay to work from home. This finding suggests additional welfare benefits from the work-from-home technology boon than higher consumption.

Our paper also relates to a more recent literature investigating the long-term effects of the COVID crisis on work and cities. Our paper is perhaps most closely related to Delventhal, Kwon, and Parkhomenko (2020). Delventhal, Kwon, and Parkhomenko (2020) model the effect of an exogenous increase in the share of market work done from home on city structure. In addition to modeling the driving engine of work from home, our model captures heterogeneity in the skill level of workers that can work from home.

Finally, our work relates to how cities respond to shocks in the short-run and long-run. Ouazad (forthcoming) surveys this literature. Our model predicts the trend towards suburbanization Ouazad (forthcoming) finds. The evidence suggests that natural disasters tend to have only transitory effects on city structure (Davis and Weinstein, 2002; Ouazad, forthcoming) but that factors that influence productive capacity, such as transportation, tend to have permanent effects (Bleakley and Lin, 2012; Brooks and Lutz, 2019). Our model predicts that the short-run shock to productivity at the office will have long-lasting effects on city structure.

We present our model in the next section. Section 3 describes how we estimate the elasticity of substitution of working at home and working at the office and calibrate the other parameters of the model. In section 4 we run counterfactual experiments of the model, showing how changes to work-at-home technology affect the allocation of time of high-skill, incomes of high- and low-skill workers, and office and residential rents. Section 5 concludes.

2 Model

A measure 1 of households live in a large metropolitan area that we call a city. A fraction π of workers are high-skill and $1 - \pi$ are low-skill. Low-skill workers differ from high-skill workers in the model along a number of dimensions. The most important difference is that we allow high-skill workers to optimally allocate their time between working at the office and working at home, but low-skill workers only work at the office. Although this difference is extreme, it highlights the fact that working from home is much more common among college-educated workers.[1] Unless otherwise specified, variables and parameters specific to high-skill workers have a superscript of 1 and variables and parameters specific to low-skill workers have a superscript of 0.

2.1 Low-Skill Workers

We start by studying the decision problem of low-skill workers. All low-skill workers work for firms operating in the CBD. Low-skill workers choose where to live and how much labor to supply. Firms pay w^0 per unit of low-skill labor that is supplied, so low-skill households living in location n working b_n hours in the CBD earn annual income of $w^0 b_n$.

Households receive utility from consumption, housing, leisure, and amenities specific to a location. Denote these variables for low-skill workers living in location n as n as c_n^0, h_n^0, ℓ_n^0, and χ_n^0. Low-skilled households living in n receive utility of

$$\nu^0 \left[\log \chi_n^0 \; + \; \left(1-\alpha^0\right) \log c_n^0 \; + \; \alpha^0 \log h_n^0 \; + \; \psi^0 \log \ell_n^0\right]. \tag{1}$$

Non-housing consumption is is equal to labor income less housing expenditures, $c_n^0 = w^0 b_n - r_n h_n^0$, where r_n is the rental price of one unit of housing at location n. Leisure is equal to time not spent commuting or working in the CBD, $\ell_n^0 = 1-(1+t_n^0)b_n$, where t_n^0 is the commuting time required for each unit of work in the CBD for low-skill workers. We discuss ν^0 later; for now it can be ignored. α^0 captures the benefit of more housing relative to non-housing consumption and ψ^0 captures the benefit of more leisure.

[1]See, for example, Arbogast, Gascon, and Spewak (2019), Dingel and Neiman (2020), Mas and Pallais (2020), and Papanikolaou and Schmidt (2020).

The optimal quantities of housing and time spent working in the CBD solve

$$\max_{h_n^0, b_n} \nu^0 \left[\log \chi_n^0 + \left(1 - \alpha^0\right) \log \left(w^0 b_n - r_n h_n^0\right) + \alpha^0 \log h_n^0 + \psi^0 \log \left(1 - (1 + t_n^0) b_n\right) \right].$$

The first-order conditions are

$$\begin{aligned} b_n &= \left(\frac{1}{1+t_n^0}\right)\left(\frac{1}{1+\psi^0}\right) \\ h_n^0 &= \alpha^0 w^0 b_n / r_n \end{aligned}$$

implying $c_n^0 = (1 - \alpha^0)\, w^0 b_n$. Optimized utility for low-skill workers living in location n is thus

$$u_n^0 = \nu^0 \left[\log \chi_n^0 - \log(1 + t_n^0) - \alpha^0 \log r_n + \zeta^0 \right]$$

where ζ^0 is a constant that depends on α^0, ψ^0, and w^0. Note that utility is increasing in amenities χ^0, decreasing in commute times t_n^0, and decreasing in rental prices r_n.

We allow low-income households to vary in their preferences for living in location n. For a particular low-income household i, the utility of living in n is

$$u_{ni}^0 = u_n^0 + e_{ni}$$

where e_{ni} is assumed to vary across households i and locations n. Since e_{ni} is additive, it does not affect any decisions conditional on residing in location n. We assume that e_{ni} is drawn from the Type 1 Extreme Value distribution.

Household i chooses its optimal location of residence n_i^* to satisfy

$$n_i^* = \arg\max_{n=1,\ldots,N} \left\{ u_{ni}^0 \right\}$$

where N is the number of locations in the city where the agent can live. Define the variable U^0, proportional to expected utility for low-skill households, as

$$U^0 \;=\; \log \sum_N e^{u_n^0}.$$

Due to the properties of the Type 1 Extreme Value distribution, the probability low-skill household i lives in specific location n' is

$$f_{n'}^0 \;=\; e^{u_{n'}^0} / e^{U^0}$$

and log relative probabilities over location choice between locations n' and n has the simple expression

$$\begin{aligned} \log\left(f_{n'}^0 / f_n^0\right) \;&=\; u_{n'}^0 - u_n^0 \\ &=\; \nu^0 \left[\log\left(\chi_{n'}^0 / \chi_n^0\right) \;-\; \log\left(\frac{1+t_{n'}^0}{1+t_n^0}\right) \;-\; \alpha^0 \log\left(r_{n'}/r_n\right)\right]. \end{aligned}$$

The population of low-skill workers is decreasing in commuting costs, decreasing in rental prices, and increasing in amenities. The parameter ν^0 pins down the responsiveness of the low-skill population with respect to differences in amenities or commuting costs and, given this, α^0 pins down the responsiveness of the population with respect to rental prices.

2.2 High-Skill Workers

High-skill workers can work at home or in the office which we assume (for convenience) is located in the CBD. The total amount of effective labor that a high-skill worker living in location n supplies to a firm, y_n, is a CES aggregate of effective labor while working from home, y_n^h, and effective labor while working at the office, y_n^b, specifically

$$
(2) \qquad y_n = \left[\left(y_n^b\right)^{\rho} + \left(y_n^h\right)^{\rho} \right]^{1/\rho}
$$

$\rho \leq 1$ determines the elasticity of substitution of effective labor at home and at the office in creating units of total effective labor. Firms pay w^1 per unit of total effective high-skill labor and total income to high-skill workers supplying y_n units of effective labor is $w^1 y_n$.

Effective labor at home and in the CBD are generated using raw hours worked l and space s according to

$$
(3) \qquad y_n^b = A^b \left(s_n^b\right)^{\theta} \left(l_n^b\right)^{1-\theta}
$$

$$
(4) \qquad y_n^h = A^h \left(s_n^h\right)^{\theta} \left(l_n^h\right)^{1-\theta}
$$

where s_n^b and s_n^h refer to space rented in the CBD and space rented at home that is strictly dedicated to work (such as a home office), respectively, and l_n^b and l_n^h refer to hours worked at the office in the CBD and hours worked at home. θ is the share of space in the production process, which is identical for the home and the CBD. A^b and A^h are total factor productivity for effective labor at the firm and at home for high-skill households. Households take the values of A^b and A^h as given.

Denote consumption, housing, leisure, and amenities in location n for high-skill households as c_n^1, h_n^1, ℓ_n^1, and χ_n^1. Utility over these variables for high-skill workers is[2]

$$\nu^1 \left[\log \chi_n^1 \; + \; \left(1-\alpha^1\right) \log c_n^1 \; + \; \alpha^1 \log h_n^1 \; + \; \psi^1 \log \ell_n^1\right]. \tag{5}$$

High-skill workers maximize utility by choosing consumption, housing, leisure, hours to work in the CBD and at home, and office space to rent at the CBD and at home. Denote r^b as the rent per unit of office space in the CBD. For the time being, we suppress location subscripts (the n) and high-skill superscripts (the 1) to keep notation manageable. Thus, at any given location, high-skill households maximize utility by solving

$$\max_{y,y^b,y^h,l^b,l^h,s^b,s^h,c,h,\ell} \nu \left[\log \chi \; + \; (1-\alpha) \log c \; + \; \alpha \log h \; + \; \psi \log \ell\right]$$

subject to

$$\begin{aligned}
0 &= \mu_c \left[wy - c - r^b s^b - r\left(s^h + h\right)\right] \\
0 &= \mu_y \left\{\left[\left(y^b\right)^\rho \; + \; \left(y^h\right)^\rho\right]^{1/\rho} \; - \; y\right\} \\
0 &= \mu_b \left[A^b \left(s^b\right)^\theta \left(l^b\right)^{1-\theta} \; - \; y^b\right] \\
0 &= \mu_h \left[A^h \left(s^h\right)^\theta \left(l^h\right)^{1-\theta} \; - \; y^h\right] \\
0 &= \mu_\ell \left[1 \; - \; (1+t)\, l^b \; - \; l^h \; - \; \ell\right]
\end{aligned}$$

where μ_c, μ_y, μ_b, μ_h, and μ_ℓ are Lagrange multipliers.

[2] In our calibration we set $\alpha^0 > \alpha^1$. This is an analytically tractable way to capture non-homothetic preferences in housing consumption, i.e., that poor people spend a larger fraction of their income on housing. Although Davis and Ortalo-Magné (2011) argue that the expenditure share on rent for the median renter is constant across cities and over time, a large number of studies find that, in the cross-section of people, a 1% increase in income results in a much less than 1% increase in housing expenditure. See, for example, Rosen (1979), Green and Malpezzi (2003), Glaeser, Kahn, and Rappaport (2008), and Rosenthal (2014).

The first-order conditions are

$$
\begin{aligned}
y:& \qquad & \mu_y &= w\mu_c \\
y^b:& & \mu_b &= \mu_y y^{1-\rho}\left(y^b\right)^{\rho-1} \\
y^h:& & \mu_h &= \mu_y y^{1-\rho}\left(y^h\right)^{\rho-1} \\
l^b:& & \mu_\ell\left(1+t\right) &= \mu_b\left(1-\theta\right)\left(y^b/l^b\right) \\
l^h:& & \mu_\ell &= \mu_h\left(1-\theta\right)\left(y^h/l^h\right) \\
s^b:& & \mu_c r^b &= \mu_b\theta\left(y^b/s^b\right) \\
s^h:& & \mu_c r &= \mu_h\theta\left(y^h/s^h\right) \\
c:& & \mu_c &= \left(1-\alpha\right)\nu/c \\
h:& & \mu_c r &= \alpha\nu/h \\
\ell:& & \mu_\ell &= \psi\nu/\ell.
\end{aligned}
$$

From the FOCs for y^b and y^h we get

$$
\frac{\mu_b}{\mu_h} = \left(\frac{y^b}{y^h}\right)^{\rho-1}
$$

and the FOCs for s^b and s^h imply

$$
\frac{s^b}{s^h} = \left(\frac{\mu_b}{\mu_h}\right)\left(\frac{y^b}{y^h}\right)\left(\frac{r^b}{r}\right)^{-1} = \left(\frac{y^b}{y^h}\right)^{\rho}\left(\frac{r^b}{r}\right)^{-1}. \tag{6}
$$

Now use the production function for y^b and y^h to determine

$$
\begin{aligned}
\frac{y^b}{y^h} &= \left(\frac{A^b}{A^h}\right)\left(\frac{s^b}{s^h}\right)^{\theta}\left(\frac{l^b}{l^h}\right)^{1-\theta} \\
&= \left(\frac{A^b}{A^h}\right)\left(\frac{y^b}{y^h}\right)^{\rho\theta}\left(\frac{r^b}{r}\right)^{-\theta}\left(\frac{l^b}{l^h}\right)^{1-\theta} \\
\left(\frac{y^b}{y^h}\right)^{1-\rho\theta} &= \left(\frac{A^b}{A^h}\right)\left(\frac{r^b}{r}\right)^{-\theta}\left(\frac{l^b}{l^h}\right)^{1-\theta} \\
\rightarrow \frac{y^b}{y^h} &= \left(\frac{A^b}{A^h}\right)^{\frac{1}{1-\rho\theta}}\left(\frac{r^b}{r}\right)^{\frac{-\theta}{1-\rho\theta}}\left(\frac{l^b}{l^h}\right)^{\frac{1-\theta}{1-\rho\theta}}. \qquad (7)
\end{aligned}
$$

Return to the FOCs for l^b and l^h

$$
\begin{aligned}
\frac{l^b}{l^h} &= \left(\frac{\mu_b}{\mu_h}\right)\left(\frac{y^b}{y^h}\right)(1+t)^{-1} \\
&= \left(\frac{y^b}{y^h}\right)^{\rho}(1+t)^{-1} \\
&= \left(\frac{A^b}{A^h}\right)^{\frac{\rho}{1-\rho\theta}}\left(\frac{r^b}{r}\right)^{\frac{-\rho\theta}{1-\rho\theta}}\left(\frac{l^b}{l^h}\right)^{\frac{\rho(1-\theta)}{1-\rho\theta}}(1+t)^{-1} \\
\rightarrow \left(\frac{l^b}{l^h}\right)^{\frac{1-\rho}{1-\rho\theta}} &= \left(\frac{A^b}{A^h}\right)^{\frac{\rho}{1-\rho\theta}}\left(\frac{r^b}{r}\right)^{\frac{-\rho\theta}{1-\rho\theta}}(1+t)^{-1}
\end{aligned}
$$

which gives us

$$
\frac{l^b}{l^h} = \left(\frac{A^b}{A^h}\right)^{\frac{\rho}{1-\rho}}\left(\frac{r^b}{r}\right)^{\frac{-\rho\theta}{1-\rho}}(1+t)^{\frac{-(1-\rho\theta)}{1-\rho}}. \tag{8}
$$

Equation (8) yields an expression for l^b/l^h, which we use with equation (7) to solve for y^b/y^h given prices r^b and r. Given y^b/y^h, r^b, and r we use equation (6) to solve for s^b/s^h.

Next, we combine the FOCs for l^b, l^h, and ℓ to show that leisure is a constant. Note that

$$
\mu_\ell\left[(1+t)\,l^b + l^h + \ell\right] = \psi\nu + (1-\theta)\left[\mu_b y^b + \mu_h y^h\right].
$$

Impose the time constraint and use the FOCs for y^b and y^h to get

$$
\begin{aligned}
\mu_\ell &= \psi\nu + (1-\theta)\,\mu_y y^{1-\rho}\left[\left(y^b\right)^{\rho} + \left(y^h\right)^{\rho}\right] \\
&= \psi\nu + (1-\theta)\,\mu_y y^{1-\rho}\left[y^{\rho}\right] \\
&= \psi\nu + (1-\theta)\,\mu_y y \\
&= \psi\nu + (1-\theta)\,\mu_c w y.
\end{aligned}
$$

Now consider the FOCs for c, h, s^h and s^b

$$\mu_c \left[c + r\left(s^h + h\right) + r^b s^b\right] = (1-\alpha)\nu + \alpha\nu + \theta\left[\mu_b y^b + \mu_h y^h\right].$$

Impose the budget constraint to get

$$\begin{aligned} \mu_c wy &= \nu + \theta\left[\mu_b y^b + \mu_h y^h\right] \\ &= \nu + \theta \mu_c wy \\ \rightarrow \mu_c wy &= \frac{\nu}{1-\theta} \end{aligned} \tag{9}$$

which implies $\mu_\ell = \nu(1+\psi)$. Insert this into the first order condition for ℓ to uncover

$$\ell = \frac{\psi}{1+\psi}$$

yielding that leisure is constant and independent of n. Given a value of the parameter ψ, equation (8) completely characterizes how the household uses time not spent enjoying leisure.

The expression for $\mu_c wy$ in equation (9) allows us to directly solve for consumption, housing, and spending on office space in the CBD and at home as a function of labor income (from the first-order conditions):

$$\begin{aligned} c &= (1-\theta)(1-\alpha) wy \\ rh &= (1-\theta)\alpha wy \\ r^b s^b + r s^h &= \theta wy. \end{aligned} \tag{10}$$

Given a solution for s^b/s^h, and given solutions for l^b and l^h, equation (10) enables us to solve for s^b and s^h separately. Rewrite (10) as

$$s^h \left[r^b \left(\frac{s^b}{s^h} \right) + r \right] \quad = \quad \theta w y.$$

Note that all the terms in the brackets in the left-hand side are functions of the parameters since we can insert equation (8) into equation (7) and in turn get s^b/s^h as a function of the model parameters using equation (6). From the production function(s), we can then write

$$\theta w y \quad = \quad \theta w \left(s^h \right)^\theta \left[\left(A^b \left(\frac{s^b}{s^h} \right)^\theta \left(l^b \right)^{1-\theta} \right)^\rho + \left(A^h \left(l^h \right)^{1-\theta} \right)^\rho \right]^{1/\rho}.$$

Combining these last two equations gives an expression for s^h that is a function of all terms that are known,

$$s^h \quad = \quad \left\{ \frac{\theta w \left[\left(A^b \left(\frac{s^b}{s^h} \right)^\theta \left(l^b \right)^{1-\theta} \right)^\rho + \left(A^h \left(l^h \right)^{1-\theta} \right)^\rho \right]^{1/\rho}}{\left[r^b \left(\frac{s^b}{s^h} \right) + r \right]} \right\}^{\frac{1}{1-\theta}}.$$

Once we know s^h, we also know s^b. Given knowledge of l^b, s^b, l^h, and s^h, we therefore know income wy and the entire allocation and utility for high-skill workers at any location n.

To continue, we reintroduce location subscripts and worker-skill superscripts. Denote maximized utility for high-skill workers at location n as u_n^1. Similar to low-skill workers, each high-skill household j has a specific additive preference for living in location n, e_{nj}, such that utility of living in n for household j is

$$u_{nj}^1 \quad = \quad u_n^1 \quad + \quad e_{nj}.$$

Since e_{nj} is an additive shock, it does not affect any decisions conditional on residing in location n. As with low-skill workers, we assume that e_{nj} is drawn iid from the Type 1 Extreme Value distribution. Household j chooses its optimal location of residence n_j^* to satisfy

$$n_j^* = \underset{n=1,\ldots,N}{\arg\max} \left\{ u_{nj}^1 \right\}.$$

Denote the probability a high-skill worker optimally chooses to live in location n as f_n^1. The log relative probability high-skill workers choose location n' as compared to n is equal to

$$\log\left(f_{n'}^1 / f_n^1\right) = u_{n'}^1 - u_n^1$$

which we cannot reduce further analytically.

2.3 Wage Rates per Effective Hour

Define the total hours of all low-skill workers as $B = \sum_n f_n^0 b_n$ and the total effective hours of all high-skill workers as $Y = \sum_n f_n^1 y_n$. A representative firm aggregates these quantities and produces a final good according to

$$\mathcal{O} = \left[B^\omega + \lambda Y^\omega\right]^{\frac{1}{\omega}}.$$

The firm chooses B and Y to maximize profits according to

$$\left[B^\omega + \lambda Y^\omega\right]^{\frac{1}{\omega}} - w^0 B - w^1 Y.$$

The first-order conditions of this problem yield an expression for payment per unit of effective hours for both low- and high-skill

$$\begin{aligned} w^0 &= \mathcal{O}^{1-\omega} (B)^{\omega-1} \\ w^1 &= \mathcal{O}^{1-\omega} \lambda (Y)^{\omega-1} \end{aligned}$$

implying

$$\frac{w^1}{w^0} = \lambda \left(\frac{Y}{B}\right)^{\omega-1}. \tag{11}$$

2.4 Technology and Commuting Processes

Although our model is static, in our counterfactual experiments we solve for different steady states of the model in which the variables governing the relative technology of working at home and in the office, A_h and A_b, may be different than in our baseline calibration. One important consideration is whether we should expect the level of work-at-home technology, A_h, to change in response to a surge in the quantity of people that have worked at home (due to the pandemic). To allow for this possibility, we specify

$$A^h = \bar{A}^h \left(L_h^{max}\right)^{\delta_h} \tag{12}$$

where L_h^{max} is the highest amount of time in aggregate that high-skill agents spent working at home in any previous year.[3] This captures the idea that if suddenly many more people have had experience working at home, then all workers will be more productive in the future at working at home.[4]

[3]Note that L_h^{max} is bounded below by 0 and above by $\pi / \left(1 + \psi^1\right)$.

[4]For example, a home fitness equipment salesperson will find more value in adopting work-from-home technology if she expects to be able to exhibit her product via teleconference than if she only anticipates other salespeople to have had experience with videoconference technology. Similarly, a tax preparer may invest in work-from-home technology if he anticipates that most of his clients will be

Additionally, high-skill worker productivity at the office, A_b, may be subject to agglomeration externalities, such that the quantity of workers at the CBD directly affects A_b. Define the aggregate quantity of hours of high-skill workers in the CBD as $L_b = \pi \sum_n f_n^1 l_b^n$.[5] We specify

$$A^b = \bar{A}^b L_b^{\delta_b} \tag{13}$$

with $\delta_b \geq 0$.

Finally, we allow for the possibility of congestion externalities in commuting, and that low-skill workers may face longer commute times to the CBD than high skill at each residential location n. We specify

$$\begin{aligned} t_n^1 &= \bar{t}_n \left(B + L_b\right)^\gamma \\ t_n^0 &= \kappa\, t_n^1 \quad \text{with } \kappa \geq 1. \end{aligned}$$

With this specification $\gamma \geq 0$ captures congestion externalities and $\bar{t}_n$ can vary with location, but the percentage change in commuting costs due to the congestion externality is constant.

Note that in the presence of agglomeration and congestion externalities, the equilibrium we compute is likely inefficient because the household does not consider the impact of his or her decisions on the productivity and commuting times of others. If agglomeration economies are exclusively at the level of the firm, the firm can internalize the externality. However, if there are significant externalities at the city-level, such as the sort documented by Atkin, Chen, and Popov (2020), there may be a role for public policy to improve expected utility. A large body of earlier work suggests agglomeration economies operate across firms within the same industry and across industries. Many of these agglomeration economies require face-to-face interaction

willing to meet virtually and transmit documents electronically.

[5]Like L_h^{max}, L_b is bounded below by 0 and above by $\pi / \left(1 + \psi^1\right)$.

to achieve rather than proximity merely entailing a reduction in trade costs. Glaeser (2012) and Combes and Gobillon (2015) review this literature.

3 Parameterizing the Model

With the exception of δ_h, we estimate or calibrate the parameters of the model to data prior to the onset of COVID.

3.1 Estimating the Elasticity of Substitution between Home and Office Work

The parameter ρ governs the elasticity of substitution (EOS) between home and office work and is new to the literature. Our estimation strategy for ρ builds on Equation (8), which implies that the log-odds of commuting are linear in log-commuting costs, $\log(1+t)$,

$$\log\left(\frac{l^b}{l^h}\right) = \frac{\rho}{1-\rho}\log\left(\frac{A^b}{A^h}\right) + \frac{-\rho\theta}{1-\rho}\log\left(\frac{r^b}{r}\right) + \frac{-(1-\rho\theta)}{1-\rho}\log\left(1+t\right) \tag{14}$$

with a slope coefficient (third term) of $\Psi \equiv \dfrac{\partial \log(l^b/l^h)}{\partial \log(1+t)} = \frac{-(1-\rho\theta)}{1-\rho}$.

Conceptually, one can think of l^b as typical days worked in the office per week or month and l^h as typical days worked at home over the same period. If we define $x = l^b/l^h$, then the probability that a person works in the office on any given day is equal to $x/\left(1+x\right)$. This transformation allows us to use survey data on the fraction of days spent working at home versus in the office to estimate ρ for reasons we explain next.

Define $\overline{\mathcal{C}}_i$ as the fraction of days individual i reports working in the office. Then, we can write the estimating version of Equation (14) as

$$
\begin{aligned}
E(\overline{\mathcal{C}}_i) &= \frac{\exp\left(\log\left(\frac{l^b}{l^h}\right)\right)}{1+\exp\left(\log\left(\frac{l^b}{l^h}\right)\right)} \\
E(\overline{\mathcal{C}}_i) &= \Lambda\left(\log\left(l^b/l^h\right)\right) \\
E(\overline{\mathcal{C}}_i) &\approx \Lambda\Big(\beta_0 + X_i'\beta_1 + \Psi\log\left(1+t_i\right)\Big)
\end{aligned} \tag{15}
$$

where $\Lambda(.)$ is the logistic function. The transformation is required because some individuals in our data report that they never work at home. Even if our theory predicts everyone spends at least some some time at home, when surveyed over a small-enough time window a respondent may not have worked at home at all. For these individuals, $\mathcal{C}_i$ is well defined but $\log\left(l^b/l^h\right)$ is not.

We account for unmodeled heterogeneity in the relative productivity of work from home and work at the office across people by replacing the two leading terms in (14) with a function of observable characteristics (X_i). We include age, age^2, a female indicator, age-female and age^2-female interactions, race, marital status, two-digit industry dummies, and two-digit occupation dummies in X_i. The main regressor of interest is $\log(1+t_i)$, which must vary across households (conditional on X_i) to identify Ψ.

3.1.1 Data

We estimate the parameters of (15) using data from the 2017-2018 Current Population Survey (CPS), the American Time Use Survey (ATUS), and the Leave and Job Flexibility (LJF) module of the CPS. The ATUS and LJF are both CPS submodules. Respondents provide time a diary of activities on one randomly chosen day. The ATUS data provide a record of commute duration for cases where a commute occurs on the observation day. The LJF sample is a subsample of ATUS respondents. LJF asks questions focusing on workplace leave policies and job flexibility, including whether respondents have the ability to work from home and the frequency of home work.

We merge ATUS and JTW records at the individual level to create a dataset containing both commute times and frequencies of work at home. There are two main challenges with using these data. First, following the merge, we restrict to individuals who were observed commuting on their randomly selected ATUS observation day. This necessary sample restriction introduces non-representativeness to our merged sample. Given that we exclude from the sample observations where people are not commuting on the ATUS observation day, the probability of an individual i being represented in our sample is increasing in the probability that i commutes on any given day. We correct for this by reweighting the sample. The LJF survey collects information on the fraction of days that each individual commutes; denote this fraction $\overline{\mathcal{C}}_i$. Given the probability that the respondent is included in our sample is (effectively) equal to the fraction of that individual's days that involve a commute, we reweight to undo this selection by setting sampling weights equal to the inverse of this fraction, $IPW_i = 1/\overline{\mathcal{C}}_i$.

Second, there is likely significant measurement error in the reporting of commute times. For example, over 90% of people report a commute time that is a multiple of 5 minutes, and there are large masses at 15 and 30 minutes. We use two approaches to correct for bias due to measurement error. The first is an instrumental variables approach that exploits the fact that we observe multiple reported commute times for the majority of individuals in our sample. We compute the two measures of commuting cost using $t_{i1} = \frac{2\times\text{commute time}_{i1}\text{ (minutes)}}{8\times60}$ and $t_{i2} = \frac{2\times\text{commute time}_{i2}\text{ (minutes)}}{8\times60}$ defining the "commute times" as the lengths of the two longest-duration activity intervals classified as "time spent traveling for work" in the ATUS time diary. For individuals who report only one "time spent traveling for work" interval, t_{i2} is missing. Using one measure as an IV for the other is a common approach to addresses measurement errors under the assumption that the measurement errors from the two measures are uncorrelated.

Two striking patterns in the commute-time data, shown in Figure A.2 of the Appendix, cause us to suspect that the measurement errors may, in fact, be correlated. First, shown in the top panel of the figure, 51% of individuals with two observed commutes report the exact same commute time. Second, shown in the bottom panel, most commute times appear to be rounded, with 91% being a multiple of 5 minutes and 46% being a multiple of 15 minutes. Based on this evidence, we believe it is likely the measurement error of two reported commutes is positively correlated.[6] Therefore, our second approach to addressing measurement error involves correcting non-IV estimates of ψ using an analytically-derived adjustment that is based on an assumed value of the correlation of the measurement errors of the two reported commutes. With this approach, we are able to assess the sensitivity of our estimates of ψ to the correlation of the measurement errors.

3.1.2 Estimation Details

We use a GMM estimator to compute estimates of Ψ. We first compute estimates that do not correct for measurement error in reported computing times. We then use a related IV version of the estimator to compute measurement-error-corrected estimates. The moments we target for estimation are based on the error term given by the difference between each individual's reported fraction of days spent in the office and the prediction given by Equation (15). Under a given parameterization (Ψ, β) this prediction error can be written

$$\epsilon_i(\Psi, \beta) = \overline{C}_i - \Lambda\Big(\beta_0 + X_i'\beta_1 + \Psi \log\big(1 + t_{i1}\big)\Big).$$

[6]For example, a person with two realized commutes of 26 minutes and 27 minutes might report 30 minutes for both commutes.

The GMM estimator with no measurement error correction is based on the moments

$$
\begin{aligned}
\widehat{m}_0(\Psi,\beta) &= \sum_i \epsilon_i(\Psi,\beta) \\
\widehat{m}_1(\Psi,\beta) &= \sum_i X_{i1}\epsilon_i(\Psi,\beta) \\
&\vdots \\
\widehat{m}_K(\Psi,\beta) &= \sum_i X_{iK}\epsilon_i(\Psi,\beta) \\
\widehat{m}_{K+1}(\Psi,\beta) &= \sum_i \log(1+t_{i1})\epsilon_i(\Psi,\beta)
\end{aligned} \tag{16}
$$

where K is the length of X_i. Estimation is based on the moment condition, $E[\widehat{m}(\Psi,\beta)] = 0$, where

$$
\widehat{m}(\Psi,\beta) = \begin{bmatrix} \widehat{m}_0(\Psi,\beta) \\ \widehat{m}_1(\Psi,\beta) \\ \vdots \\ \widehat{m}_{K+1}(\Psi,\beta) \end{bmatrix}
$$

and the GMM estimator is

$$
(\widehat{\Psi}^{GMM}, \widehat{\beta}^{GMM}) = \underset{(\Psi,\beta)}{\arg\min} \; \widehat{m}'(\Psi,\beta)\, \mathcal{W}\, \widehat{m}(\Psi,\beta) \tag{17}
$$

where $\mathcal{W}$ is an optimal weighting matrix.

This GMM framework also directly facilitates our IV strategy for accounting for measurement error. We correct for measurement error using two approaches, both of which rely on the bias due to measurement error in our logistic setting being similar to that which arises in the linear regression framework. In the appendix, we show that over the relevant range of commute times and a high probability of commuting similar to what we observe in the data, the logistic function is close to linear such that a linear approximation is reasonable.

Both approaches exploit the fact that many people report more than one commute. We use one commute for the same individual as an instrument for the other commute. This corrects for the measurement error within an individual that is uncorrelated across trips. For example, suppose an individual recalls that the afternoon commute was 18 minutes while only recalling that the morning commute was approximately 20 minutes. Alternatively, suppose an individual runs an errand on the way home from work and thus misreports the afternoon commute time because of inclusion of the errand. The morning commute is correlated with the true commute time but uncorrelated with the extra errand time.

Our first approach to correcting for correcting for measurement error constructs the GMM-IV estimator by replacing the orthogonality condition, moment $K+1$, with the IV analog,

$$\widehat{m}_{K+1}(\Psi, \beta) \quad = \quad \sum_i \log(1+t_{i2})\epsilon_i(\Psi, \beta). \tag{18}$$

That is, identification of Ψ is based on the orthogonality of the second-commute-time IV $\log(1+t_{i2})$ with the prediction error calculated using $\log(1+t_{i1})$. To maximize efficiency, we allow each individual in our sample to contribute two observations for the IV estimator. For one observation, we treat the first commute time measurement as the regressor $\log(1+t_{i1})$ and the second commute time measurement as the instrument $\log(1+t_{i2})$, and for the second observation we reverse the roles of the two measures.

Our second strategy to account for measurement error involves applying an analytical correction to the estimate of Ψ from the GMM moments in Equation (16). We derive the correction by applying the analytical expression for the magnitude of attenuation bias in the linear regression framework,

$$E[\widehat{\Psi}^{GMM}] \approx \Psi \times \left(\frac{var(\overbrace{x_i^*}^{\text{true value}})}{var(\underbrace{x_{i1}}_{\text{measured value}})} \right) \tag{19}$$

where, for compactness of notation, we have substituted $x_i^* = log(1 + t_i)$ for the true value of the mismeasured covariate and $x_{i1} = log(1 + t_{i1})$ and $x_{i2} = log(1 + t_{i2})$ for the measurements. We write the measurements as

$$\begin{aligned} x_{i1} &= x_i^* + e_{i1} \\ x_{i2} &= x_i^* + e_{i2} \end{aligned}$$

$$var\left(\begin{bmatrix} e_{i1} \\ e_{i2} \end{bmatrix}\right) = \begin{bmatrix} \sigma_e^2 & \rho_e \sigma_e^2 \\ \rho_e \sigma_e^2 & \sigma_e^2 \end{bmatrix}.$$

The measurement errors e_{i1} and e_{i2} are uncorrelated with x_i^* but are potentially correlated with one another with correlation coefficient $\rho_e > 0$.

We construct the bias-corrected estimator by multiplying the naive GMM estimator by the inverse of an estimate of the attenuation bias

$$\begin{aligned} \widehat{\Psi}^{BC} &= \widehat{\Psi}^{GMM} \left(\frac{\widehat{var}(x_1)}{\widehat{var}(x^*)} \right) \\ &= \widehat{\Psi}^{GMM} \left(\frac{\widehat{var}(x_1)}{\widehat{var}(x_1) - \widehat{var}(e)} \right). \end{aligned}$$

Finally, noting that

$$\begin{aligned} var(x_{i1}) &= \sigma_{x^*}^2 + \sigma_e^2 \\ cov(x_{i1}, x_{i2}) &= \sigma_{x^*}^2 + \rho_e \sigma_e^2 \end{aligned}$$

which imply that

$$var(e_i) \quad = \quad \frac{var(x_{i1}) - cov(x_{i1}, x_{i2})}{1 - \rho_e}$$

the bias-corrected estimator is

$$\widehat{\Psi}^{BC} \quad = \quad \widehat{\Psi}^{GMM} \left(\frac{\widehat{var}(x_{i1})}{\widehat{var}(x_{i1}) - \left(\frac{\widehat{var}(x_{i1}) - \widehat{cov}(x_{i1}, x_{i2})}{1 - \rho_e} \right)} \right). \tag{20}$$

In the appendix, we present evidence from Monte Carlo experiments showing that the correction based on this approximation performs well in simulated datasets that match key moments of the commute data and with a range of correlations between the measurement errors in two reported commutes.

In Table 1, we report GMM estimates of ψ, the value of ρ after imposing $\theta = 0.18$, and the implied elasticity of substitution (EOS) between working at home and in the office. Columns 1 and 2 report GMM estimates without correcting for measurement error without (column 1) and with (2) demographic controls and industry and occupation fixed effects. The sample in these columns is anyone that reports at least one commute. For the 1,203 commuters that report two commutes, we create two records, one for each commute time reported. We include both these records in our estimation and allocate 50% of the IPW to each of them. These columns show that when we do not correct estimates for measurement error, the estimate of the EOS is about 3.0. Column (3) shows estimation results resulting from a simple attempt to remove observations that may obviously be contaminated with measurement error: We remove from the sample individuals who report two commutes that differ by at least 20 minutes. This removes 147 observations, 8.3 percent of the sample, and boosts the estimate of the EOS to about 3.5.

Column 4 shows our GMM estimate when we restrict the sample to individuals who report at least two commutes, 1,203 respondents, and column 5 shows our IV-corrected GMM estimates from this sample based on the moment condition shown in equation (18). The IV correction increases the coefficient estimate by a factor of nearly 1.6, from -2.54 to -3.85, raising the EOS from 2.9 to 4.5.

Columns 6-9 show the results of the analytic correction for measurement error shown in equation (20) when we use as a baseline the GMM estimates shown in column 2. When we assume the two measurement errors are uncorrelated, column 6, the estimate of ψ increases by a factor of 1.39, from -2.78 to -3.85, and the associated EOS rises from 3.18 to 4.47. As the assumed correlation of the measurement error rises, from 0.1 in column 7 to 0.25 in column 8 to 0.50 in column 9, the estimate of ψ increases in absolute value and the EOS increases from 4.68 (column 7) to 5.16 (column 8) to 7.37 (column 9).

In what follows, we set our baseline estimate of $\rho = 0.80$, implying an EOS of 5, corresponding to a correlation of the two measurement error terms of about 0.2. We explore the sensitivity of our results by considering alternative values for ρ of 0.667 and 0.857. This corresponds to elasticities of substitution between work at home and in the office of 3, our estimate when we do not correct for measurement error, and 7, our estimate when the correlation of measurement errors is about 0.5.

3.2 Other Parameters

3.2.1 Parameters Set Outside of Model

Table 2 summarizes our parameterization of the model when we allow for two residential zones. δ_b governs the extent of agglomeration returns in production for high-skill workers working in the CBD. We set this to 0.04 based on Davis, Fisher, and Whited

(2014) but consider the sensitivity of our results to a higher level of δ_b in Section 4.6. We set $\omega = 0.33$ such that the EOS between low-skill and high-skill labor is 1.5. This is in the middle of the range reported by Autor, Katz, and Krueger (1998). We set θ, the structure share in production, to 0.18 based on Valentinyi and Herrendorf (2008).

We set π, the fraction of workers that are high-skill, to 0.33 which is the share of US adults that are college-educated as of 2019 according to data from the U.S. Census Bureau. We set $\alpha^0 = 0.33$ and $\alpha^1 = 0.20$ to roughly match the relative size of housing of college and non-college educated workers in the 2019 American Housing Survey.[7] These values of α bracket the estimate of Davis and Ortalo-Magné (2011) of 0.24 for the median expenditure share on rents for all renting households in the United States.[8] The preference for leisure, ψ, does not impact our results since with log separable preferences leisure is a constant, independent of wage and location. For now, we set the preference for leisure to be the same for both low- and high-skill workers, $\psi^0 = \psi^1 = 0.25$.

ν measures how sensitive location choice is to variation in utility. In many models of urban economics, utility has to be the same everywhere. This is what emerges as $\nu \to \infty$. When ν is a finite number, people are willing to live in a place that provides lower utility on average because they get a good random draw of household-specific preferences e_{ni} from living in that location. We set $\nu^0 = \nu^1 = 3.3$ based on the estimates in Monte, Redding, and Rossi-Hansberg (2018).

In our benchmark calibration, we compute the quantity of space demanded in each zone and in the CBD at specific rental prices that we calibrate from data. In our counterfactual simulations, we either solve for new rental prices holding quantities

[7] The average home sizes for non-college-educated and college-educated households are 1,582 and 2,025 square feet.

[8] As a check, we compute the median of the ratio of annual gross rent to household income using data from the 2018 5-year American Community Survey, for non-college-educated and college-educated household-head, with the household head aged 21-65 and with positive rent and household income. These estimates are 0.31 and 0.23, respectively.

of space in each zone and the CBD as fixed, or solve for new quantities holding rental prices fixed. We use data from the New York City CBSA in 2015 to compute rents per square foot in the CBD and in zones 1 and 2 in the benchmark. According to Real Capital Analytics Trends, average rents per year per square foot on office property in Manhattan were \$37.89 per year. We apply a 5% cap rate to the median price per square foot residential prices by county in Galka (2016) to compute rents per square foot in each zone. We consider the Bergen NJ, Bronx NY, Hudson NJ, Kings NY, Richmond NY, Queens NY as Zone 1, \$13.26 rent per square foot per year, and all other counties as Zone 2, \$9.09 per square foot per year. We normalize r^b to 1.0 giving us prices of $r^b = 1.0$, $r_1 = 0.35$ and $r_2 = 0.24$.

3.2.2 Calibrated Parameters

We normalize $\bar{A}^b$ to 1 such that A^h captures the relative productivity of work from home for high-skill workers. Similarly, the model implicitly normalizes the labor productivity of low-skill workers to 1 such that the parameter λ in Equation (11) determines relative wages.

We set κ, the scale factor that determines relative commute times for low-skill workers, equal to 1.0: According to data from the ATUS, conditional on county of residence low-skill workers do not spend more time commuting than high-skill workers. γ captures how commuting costs for all workers rise with the number of commuters. For now, we set $\gamma = 0$.

χ_1^0, χ_1^1, χ_2^0, and χ_2^1 describe the relative average amenities low- and high-skill workers receive when living in Zones 1 and 2. We normalize $\chi_1^0 = \chi_1^1 = 1$. We calibrate the remaining free parameters of the model (χ_2^0, χ_2^1, λ, A_h, $\bar{t}_1$, and $\bar{t}_2$) to match the following moments that we exactly match in our benchmark parameterization:

1. Share of low-skill workers living in Zone 2 (χ_2^0): 35.8%

2. Share of high-skill workers living in Zone 2 (χ_2^1): 40.4%

3. Total age-adjusted income of high-skill relative to low-skill (λ): 1.8. Note that for the purposes of calibration, we measure labor income for high-skill workers as $wy - r^b s^b$ to account for the fact that, in the data, and unlike our model, firms pay for office space directly rather than workers.

4. Fraction of time spent working at home relative to time spent working in our benchmark for high-skill labor (A_h): 20%

5. High-skilled workers living in Zone 1 time spent commuting per work day ($\bar{t}_1$): 30 minutes per trip each way

6. High-skilled workers living in Zone 2 time spent commuting per work day ($\bar{t}_2$): 50 minutes per trip each way

We include in parentheses the parameter that is most closely related to the moment we are targeting although all parameters are jointly estimated.

We calculate moments (1) - (3) using the ATUS-CPS data for residents living in New York City, Washington DC, Charlotte, Pittsburgh, St. Louis, Denver, Detroit, Columbus OH, and Louisville metropolitan areas. We select these cities because they are monocentric and have sufficient population to identify the county of residency in the ATUS data. We set Zone 1 to the counties that are adjacent to the CBD and Zone 2 includes as counties not adjacent to the CBD but included in the CBSA. We set moment (4) based on the estimates from the ATUS and Mortensen and Wetterling (2020). The ATUS gives us a snapshot of a worker's day and we find that, of all employees with college-degrees, 17% of weekday work minutes are minutes worked from home. Mortensen and Wetterling (2020) more directly asks companies in Norway and Sweden "[H]ow much of the work done by the staff in your company/division was performed from remote locations/home offices 1) Pre-Covid-19, 2) During Covid-19 lockdown, and 3) Expectations Post-Covid-19." Figure 1 shows the respondents' answers. The mean share of employed persons that usually or sometimes work from home in the 15 EU countries surveyed 1995-2019 was approximately 19% in 2019 with the split being 6% "usually" working from home and 13% "sometimes" working from home. The figure shows that the share of workers that sometimes and usually work from home has trended upward in recent years, suggesting that COVID accelerated an existing trend. These data are not broken down by educational attainment and are likely a lower bound on the share of work done from home of college-educated workers.

4 Counterfactuals

We use the model to understand how the pandemic affected the economy and to forecast its long-term effects. At the onset of the pandemic, we assume productivity of working at the office, $\bar{A}^b$, falls significantly as workers require more space (and time) to produce output at the office due to social distancing and other precautionary responses. The model predicts this decline in office productivity leads to more work at home, which then raises A^h via Equation (12). At this new, higher level of A^h much more work occurs at home after the pandemic ends, even when productivity of working at the office returns to its pre-pandemic value.

4.1 Effects During the Pandemic

Column 1 of Tables 3 and 4 show simulations of the benchmark economy prior to the onset of the pandemic. We consider two counterfactual simulations for understanding how the pandemic affected the economy. In the first, we hold A^h at its baseline level but reduce $\bar{A}^b$ by 50%. This corresponds to the beginning of the pandemic when office productivity declines markedly but workers have not significantly increased their experience with working at home. Column 2 of Tables 3 and 4 displays the results of this first counterfactual. The overall decrease in A^b, shown in row (1), is slightly larger than the 50% decline in $\bar{A}^b$. This occurs because high-skill work at the office declines, reducing the contribution of agglomeration effects on productivity at the office. Hours worked at home for high-skill workers rise from 20% to 68% of total hours, shown in row (25), and rent for office space in the CBD falls to 34% of its pre-pandemic level, row (37). Residential rents, rows (38) and (39), are essentially flat due to offsetting forces: Households significantly increase their demand for home offices, rows (30) and (34), but incomes fall substantially, rows (4) and (7). Low-skill workers move from Zone 2 to Zone 1 (rows 12 and 13) and high-skill workers do the opposite, rows (15) and (16). Note that we hold the stock of space in the CBD (row 28) and both Zones (rows 29 and 33) in this counterfactual.

Next we consider a counterfactual simulation of the economy at the end of the pandemic, column 3 of Tables 3 and 4. In this counterfactual, $\bar{A}_b$ is still depressed due to social distancing but A^h (row 2) increases by 34%, from 0.453 to 0.607, such that the percentage of high-skill work that occurs from home doubles from 0.2 to 0.4 (row 25, column 4) once $\bar{A}_b$ returns to its pre-pandemic level. Row 25 shows that hours worked at home rises to 83% (column 3), from 68% at the start of the pandemic (column 2) and 20% prior to the pandemic, column 1. Comparing columns 1 and 3 for rows (30) and (34), the model predicts an increase in demand for home offices of four times in Zone 1 and three times in Zone 2. Since we fix the supply of space in each zone is assumed fixed in this counterfactual, the increase in the size of home offices is accommodated by a decrease in space used for housing, rows (31) - (32) and (35) - (36). Rents in the CBD fall to just 22% of their pre-pandemic level, row (37), and residential rents in both zones rise (rows 38 and 39). Shown in row (7), *measured* income per high-skill worker actually increases by 4.1% from the benchmark, from 5.41 to 5.63, as the increase in A_h mitigates the steep decline in the productivity of work from the office and workers pay more toward rent on their larger home offices.

4.2 Effects After the Pandemic

We consider three counterfactual experiments that bracket the possible changes to city form and the use of space after the health-related impacts of the pandemic subside such that people can start freely interacting again. In all three counterfactuals, people can freely adjust where they live, how much they spend on housing or home-office space, and how much they choose to work in the CBD or (for high-skill) in their home office. What varies between counterfactuals is the extent to which aggregate quantities or prices of space, by zone, are allowed to vary from the pre-pandemic baseline.

In the first post-COVID counterfactual, called SR in the Tables 3 and 4, we hold fixed the supply of office space in the CBD and the aggregate amount of available structures for use in housing and home-office work in each of Zones 1 and 2 (separately) at the baseline levels. In this counterfactual, we search for three market clearing prices: r^b, r_1, and r_2 such that the demand for space is equal to the supply in each zone. We think of this as a short-run response, in the sense that populations can move and the demand for space can immediately change but the supply for space has not yet responded.

In this and our other two post-COVID experiments, we keep $A^h = 0.607$, its value during the experiment for the end of the pandemic. As discussed earlier, this value of A_h generates a doubling of the share of time high-skill workers spend working the CBD relative to the baseline, from 0.2 to 0.4, which we base on the estimates from firm surveys in Mortensen and Wetterling (2020). We believe this is conservative, as Barrero, Bloom, and Davis (2020) predict a four-fold increase based on household surveys.

Comparing columns 1 and 4 of Table 3 shows that, while incomes for both types of workers rise (rows 4 and 7), the rise is more pronounced for high-skill workers such that the ratio of high-skill to low-skill income rises by 7.2%, from 1.80 to 1.93 (row 3). Low-skill wages rise because low-skill and high-skill effective hours are complementary in production: As high-skill effective hours rises, low-skill output becomes more valuable. Although high-skill workers work in the office less, there is only a slight increase in the share of high-skill workers living in Zone 2 in this counterfactual (row 16) as space has yet had a chance to adjust. Relative to the pre-pandemic benchmark, rent for office space in the CBD falls by 17% (row 37) and residential rents rise in both zones with the increase larger in Zone 2 (16.7%, row 39) than in Zone 1 (11.4%, row 38). The change in residential rents is driven by a large increase in demand for home offices (rows 30 and 34); the quantity of housing not used for home offices modestly declines for both high- and low-skill workers, rows (31) - (32) and (35) - (36).

In the second post-COVID counterfactual experiment, shown in column 5 as LR, we hold rental prices in the CBD and in both zones fixed at their baseline levels and allow the supply of space in each zone to flexibly accommodate any change in demand. We think of this as a long-run response in most areas. Once the quantity of space has adjusted, the share of high-skill hours worked from home rises even further, to 46% from 40% immediately after the pandemic (row 25). The demand for office space in the CBD declines by about 25 percent, row (28); the demand for space for all uses in Zone 1 increases by 9 percent, from 1.94 to 2.11 (row 29); and, the demand for space for all uses in Zone 2 increases by 20%, from 1.66 to 2.0 (row 33). Housing for both types of workers increases from the benchmark, as both types earn more income, but high-skill workers build even larger home offices in this environment and this makes high-skill workers even more productive at home. With this in mind, it is useful to compare the SR results, where the quantity of space in each zone is fixed and the price is flexible, to the LR results, where the price of space is fixed and quantity is flexible. In the SR, home office space approximately doubles from the pre-pandemic level, shown in rows (30) and (34). In the LR, space for home offices increases by a factor of 2.5 relative to its pre-pandemic levels.[9]

In our final post-COVID counterfactual, we hold the quantity of office space in the CBD fixed and find the rent r^b such that demand is equal to supply, but fix rents in Zones 1 and 2 at their baseline levels assuming that additional development in these zones is feasible at current prices. Column 6 shows the results of this experiment, LR Putty-Clay. This experiment recognizes that depreciation rates are sufficiently low on structures that areas with a large decline in the rental price of office space may not see a reduction in the total amount of rented space for quite some time. In this experiment, rents on office space in the CBD fall to 81% of their pre-pandemic level, row (37), and relative to the LR experiment, a smaller share of hours are worked at home, row (25), because office space is cheap in the CBD. For related reasons, the flight of high-skill workers to Zone 2 is less pronounced in column 6 than in column 5, row (16). The rise in income inequality, row (3), persists.

In all the experiments we have reported so far, consumption inequality (row 10) increases by less than income inequality (row 3). We measure consumption as the sum of expenditures on consumption and expenditures on housing not including home offices. In the post-COVID counterfactuals, wy rises for high-skill workers because they have become relatively more productive. The increase in productivity arises due to (i)

[9]We have in mind that some houses that currently do not have much of a home office will convert an empty bedroom to a home office, or will add desks and computers to unused basement space; or, some households will expand or renovate their existing home offices to make the space more productive. The point is that not every house needs to increase its space dedicated to home offices by a factor of 2.5, but rather that the space dedicated to home offices in the aggregate in the zone needs to increase.

the increase in A_h as well as (ii) the expansion of home offices. Workers are compensated for the increase in their productivity, but some of the gains in income directly offset additional expenses incurred from renting larger home offices. To match the model with data, we do not subtract expenditures on home offices from labor income as typical survey questions measuring wage and salary income do not ask respondents to net out expenditures on home offices. Measured consumption inequality does not increase as much as income inequality because rent for these home offices reduces income available for consumption for high-skill workers, and low-skill workers do not rent home offices.

4.3 A 1990 Pandemic

In Table 5 we consider a counterfactual that would correspond to the effect of the COVID pandemic if A^h was very low such that working from home was not a viable alternative for high-skill workers. This scenario corresponds to the effects of the pandemic had it happened in, say, 1990 prior to current work-at-home technology being widely available. Indeed, despite the 1918-1920 flu pandemic being an order of magnitude more lethal than that of COVID, particularly for prime-age workers, there was much less social distancing during the 1918-1920 pandemic.[10] Column 1 shows simulated outcomes of our model economy prior to the onset of the pandemic, call it 1989, and column 2 shows results once the pandemic hits. In both columns 1 and 2 we set A^h to 0.14, about 30% of its 2019 level, and then compare outcomes when we reduce $\bar{A}^b$ by 50% at the onset of the pandemic, row 1 of Table 5.

Had the pandemic occurred in 1990, the model predicts hours worked at home would have risen from 0% of 2%, row (5). Incomes for both low- and high-skill house-

[10]See Barry (2004) for a discussion of the lethality and lack of social distancing during the 1918-1920 pandemic.

holds (rows 7 and 8) would have declined by much more than implied by the counterfactual experiments for the current (2020-2021) pandemic because workers in 1990 cannot offset the decline in productivity at the CBD by working from home. Office rents in the CBD (row 12) and in both zones (rows 13 and 14) would have declined significantly due to the drop in income. Essentially, these simulations suggest worker behavior after the onset of the pandemic in 1990 would not have changed much, and the virus may have been much more costly in terms of income and much more lethal.[11]

4.4 Quantifying the Impact of Experience on A_h

In Equation (12), we specified A^h as $\bar{A}^h\left(L_h^{max}\right)^{\delta_h}$. Denote the pre-pandemic level of A^h as A_0^h and the (immediate) post-pandemic level of A^h as A_1^h. Assuming that $\bar{A}^h$ is fixed during the COVID pandemic, which is reasonable given the pandemic lasted about 12 months, we can use the simulated maximum number of hours worked from home before and during the pandemic, row (22) of Table 4, to solve for δ_h

$$\frac{A_1^h}{A_0^h} = \frac{0.607}{0.453} = \left(\frac{0.64}{0.14}\right)^{\delta_h}$$

This gives us an estimate of δ_h of 0.19, implying a 10 percent increase in aggregate hours (ever) worked at home boosts productivity of working at home for all high-skill workers by 1.9 percent.

4.5 The Role of the EOS between Home and Office Work

Figure 2 shows the sensitivity of the share of work that occurs at home, the y-axis, given log relative TFP of working at home, the x-axis, for various values of the EOS. The dashed and dotted lines correspond to EOS values of 3 and 7 and the solid line

[11] Eichenbaum et al. (2020) find that approximately 17% of virus transmissions occur in workplaces.

shows our benchmark value of 5. The figure illustrates that for our benchmark estimate of the EOS and higher values, the increase in the share of hours worked at home is nonlinear in growth of relative TFP of working from home. The nonlinearity becomes more pronounced as the EOS rises. Thus, small changes in technology can have a big impact on the location of work and urban form.

Table 6 shows how predictions of our model change depending on the EOS we choose: 3, 5, or 7. For each value of the EOS, we set A^h pre- and post-COVID such that high-skill workers spend 20% of their time working at home pre-COVID and 40% of their time working at home after COVID in the SR counterfactual. In all simulations, we assume that $\bar{A}^b$ declines by 50% during the pandemic.

Rows (2), (4), and (6) of Table 6 show the levels of A^h required to match the target values of the share of work done at home. As work from home gets more complementary with work at the office, its productivity needs to be much lower for the household to choose a low fraction of time to work from home. When the EOS is 5, we find the pre-pandemic level of A^h is 0.45 but when the EOS is 3 we have to set $A^h = 0.31$ to replicate that only 20% of high-skill hours are worked from home. When the EOS is 5, A^h has to rise by 34% (from 0.45 to 0.61) to double the hours worked from home after the pandemic ends when the EOS is 5. When the EOS is only 3, however, A^h has to increase by more than 50% to generate the increase in hours worked.

Given our method for setting A^h, Table 6 shows that the long-run implications of the COVID shock are similar regardless of the value of the EOS: 1) CBD rents fall by approximately 15-20% in both the SR and LR Putty-Clay scenarios; 2) incomes rise for both types of workers but more for high-skill workers such that income inequality increases; and 3) A^b declines due to lower agglomeration economies. At the start of COVID, column 2, residential rents actually fall in both zones when the EOS is equal to 3. This occurs because the decline in income is more pronounced with the lower value of the EOS.

4.6 Sensitivity to Agglomeration Economies in the CBD

Our benchmark parameterization sets $\delta_b = 0.04$ based on the estimates in Davis, Fisher, and Whited (2014). However, these estimates are based on data from entire metropolitan areas. To the extent that agglomeration economies may be stronger in a smaller location like a CBD, we compute counterfactuals when we set δ_b to a much higher value of 0.10. Table 7 presents these results. As with the previous counterfactual experiments, we set A^h pre- and post-COVID such that high-skill workers spend 20% of their time working at home pre-COVID and 40% of their time working at home after COVID in the SR counterfactual. Table 7 shows that this change in δ_b does not materially affect any of our main results.

4.7 Long-term Trend for Office: The Effect of Upskilling

While COVID induced a permanent change in the productivity of working from home that reduced the demand for office space in the CBD, the long-term rise in the share of the workforce with a college degree has the opposite effect on demand for office space as skilled workers demand more office space. To understand the effect of this upskilling on rents, we conduct an additional experiment in which we hold the supply of CBD office space fixed in the long run, as in our LR Putty-Clay counterfactual in column 6 of Table 4, but increase the share of high-skill workers in the population to 40%. In this scenario, we find that office rents fall to 86% of their pre-pandemic level rather than the 81% (shown in row 37 of column 6 of Table 4). Thus, an increase in the share of high-skill workers is unlikely to undo the majority of the decline in CBD office rents that we simulate in Table 4.

5 Conclusions

To understand the short and long-run effects of the COVID-19 pandemic, we have built a spatial equilibrium model that incorporates technology to work from home and to work at the office. The model illustrates that the pandemic will have very different effects in both the short-run and long-run on urban form, incomes, and rents depending on the stage of adoption of work-from-home technology.

References

ARBOGAST, I., C. S. GASCON, AND A. SPEWAK (2019): "Working from Home: More Americans Are Telecommuting," Regional Economist, Third Quarter.

ATKIN, D., K. CHEN, AND A. POPOV (2020): "The Returns to Serendipity: Knowledge Spillovers in Silicon Valley," Tech. rep., MIT.

AUTOR, D. H., L. F. KATZ, AND A. B. KRUEGER (1998): "Computing Inequality: Have Computers Changed the Labor Market?" The Quarterly Journal of Economics, 113, 1169–1213.

BARRERO, J. M., N. BLOOM, AND S. J. DAVIS (2020): "Why Working From Home Will Stick," Tech. rep., Stanford University.

BARRY, J. M. (2004): The Great Influenza: The Story of the Deadliest Pandemic in History, Penguin.

BLEAKLEY, H. AND J. LIN (2012): "Portage and Path Dependence," The Quarterly Journal of Economics, 127, 587–644.

BLOOM, N., J. LIANG, J. ROBERTS, AND Z. J. YING (2014): "Does Working from Home Work? Evidence from a Chinese Experiment," The Quarterly Journal of Economics, 130, 165–218.

BROCK, W. A. AND S. N. DURLAUF (2010): "Adoption Curves and Social Interactions," Journal of the European Economic Association, 8, 232–251.

BROOKS, L. AND B. LUTZ (2019): "Vestiges of Transit: Urban Persistence at a Microscale," The Review of Economics and Statistics, 101, 385–399.

COMBES, P.-P. AND L. GOBILLON (2015): "The Empirics of Agglomeration Economies," in Handbook of Urban and Regional Economics, ed. by W. Strange, Elsevier, vol. 5.

COMIN, D. AND M. MESTIERI (2014): "Chapter 2 - Technology Diffusion: Measurement, Causes, and Consequences," in Handbook of Economic Growth, ed. by P. Aghion and S. N. Durlauf, Elsevier, vol. 2, 565 – 622.

DAVIS, D. R. AND D. E. WEINSTEIN (2002): "Bones, Bombs, and Break Points: The Geography of Economic Activity," American Economic Review, 92, 1269–1289.

DAVIS, M. A., J. D. M. FISHER, AND T. M. WHITED (2014): "Macroeconomic Implications of Agglomeration," Econometrica, 82, 731–764.

DAVIS, M. A. AND F. ORTALO-MAGNÉ (2011): "Household Expenditures, Wages, Rents," Review of Economic Dynamics, 14, 248–261.

DELVENTHAL, M. J., E. KWON, AND A. PARKHOMENKO (2020): "How Do Cities Change When We Work from Home?" Tech. rep., Claremont McKenna College.

DINGEL, J. I. AND B. NEIMAN (2020): "How Many Jobs can be Done at Home?" Journal of Public Economics, 189, 104235.

EICHENBAUM, M., S. REBELO, AND M. TRABANDT (2020): "The Macroeconomics of Epidemics," Tech. rep., Northwestern University.

EMANUEL, N. AND E. HARRINGTON (2020): ""Working" Remotely?" Tech. rep., Harvard University.

FOSTER, A. D. AND M. R. ROSENZWEIG (2010): "Microeconomics of Technology Adoption," Annual Review of Economics, 2, 395–424.

GALKA, M. (2016): "This 3D Map Shows America's Most Expensive Housing Markets," Tech. rep., available at $http://metrocosm.com/3d-map-us-real-estate/$. Last accessed December 1, 2020.

GLAESER, E. (2012): Triumph of the City: How Our Greatest Invention Makes Us Richer, Smarter, Greener, Healthier, and Happier, New York, New York: Penguin.

GLAESER, E. L., M. E. KAHN, AND J. RAPPAPORT (2008): "Why do the Poor Live in Cities? The Role of Public Transportation," Journal of Urban Economics, 63, 1 – 24.

GREEN, R. AND S. MALPEZZI (2003): A Primer on U.S. Housing Markets and Housing Policy, Urban Press Institute.

GREENWOOD, J., A. SESHADRI, AND M. YORUKOGLU (2005): "Engines of Liberation," The Review of Economic Studies, 72, 109–133.

KATZ, M. L. AND C. SHAPIRO (1986): "Technology Adoption in the Presence of Network Externalities," Journal of Political Economy, 94, 822–841.

MAS, A. AND A. PALLAIS (2017): "Valuing Alternative Work Arrangements," American Economic Review, 107, 3722–59.

——— (2020): "Alternative Work Arrangements," Annual Review of Economics, 12, 631–658.

MCGRATTAN, E. R., R. ROGERSON, AND R. WRIGHT (1997): "An Equilibrium Model of the Business Cycle with Household Production and Fiscal Policy," International Economic Review, 38, 267–290.

MONTE, F., S. J. REDDING, AND E. ROSSI-HANSBERG (2018): "Commuting, Migration, and Local Employment Elasticities," American Economic Review, 108, 3855–90.

MORTENSEN, S. AND N. WETTERLING (2020): "Nordic Real Estate: Remote Work to Permanently Double," Tech. rep., DNB Markets.

OUAZAD, A. (forthcoming): "Resilient Urban Housing Markets: Shocks vs. Fundamentals," in Covid and Resilience, ed. by I. Linkov, B. Trump, and J. Keenan, Springer Verlag.

PAPANIKOLAOU, D. AND L. D. SCHMIDT (2020): "Working Remotely and the Supply-side Impact of Covid-19," Tech. rep., Northwestern University.

ROSEN, H. S. (1979): "Housing Decisions and the U.S. Income Tax: An Econometric Analysis," Journal of Public Economics, 11, 1 – 23.

ROSENTHAL, S. S. (2014): "Are Private Markets and Filtering a Viable Source of Low-Income Housing? Estimates from a "Repeat Income" Model," American Economic Review, 104, 687–706.

VALENTINYI, A. AND B. HERRENDORF (2008): "Measuring factor income shares at the sectoral level," Review of Economic Dynamics, 11, 820 – 835.

Table 1: GMM Estimates of the Elasticity of Substitution

			Drop			with Analytic Bias Correction			
			$\lvert x_{i1} - x_{i2} \rvert \geq 20$ mins	IV Sample	IV	$\rho_e = 0$	$\rho_e = 0.1$	$\rho_e = 0.25$	$\rho_e = 0.50$
	(1)	(2)	(3)	(4)	(5)	(6)	(7)	(8)	(9)
log(1+t)	-2.63**	-2.78**	-3.06**	-2.54*	-3.85*	-3.85**	-4.02**	-4.41**	-6.22**
	(1.21)	(1.20)	(1.53)	(1.39)	(2.11)	(1.66)	(1.74)	(1.91)	(2.69)
Implied ρ	0.67	0.69	0.72	0.65	0.78	0.78	0.79	0.81	0.86
EOS	2.99	3.18	3.51	2.87	4.47	4.47	4.68	5.16	7.37
Demog. controls	no	yes	yes	yes	yes	yes	yes	yes	yes
Industry FEs	no	yes	yes	yes	yes	yes	yes	yes	yes
Occupation FEs	no	yes	yes	yes	yes	yes	yes	yes	yes
N	1,771	1,771	1,624	1,203	1,203	1,771	1,771	1,771	1,771

Table 2: Parameterization

Param.	Description	Value	Determined
Technology:			
ρ	EOS bw home and office work = $\frac{1}{1-\rho}$	0.80	Midpoint estimate
θ	Structures share in production	0.18	Fixed
ω	EOS bw type 0 and 1 labor = $\frac{1}{1-\omega}$	0.33	Fixed
δ_b	Agglomeration economies	0.04	Fixed
κ	Relative commuting speed for type 0	1.0	Fixed
γ	Congestion externality	0.0	Fixed
$\bar{A}^b$	Productivity of working at CBD for type 1	1	Normalized
A^h	Relative productivity of work from home	0.453	Calibrated
λ	Relative productivity of high-skill worker	1.30	Calibrated
$\bar{t}_1$	Commute from Zone 1	0.125	Calibrated
$\bar{t}_2$	Commute from Zone 2	0.208	Calibrated
Rents:			
r^b	Office rent in CBD	1.0	Normalized
r_1	Residential rent in Zone 1	0.35	Fixed
r_2	Residential rent in Zone 2	0.24	Fixed
Demographics:			
π	Fraction high-skill	0.33	Fixed
Preferences:			
α^0	Housing exp. share for type 0	0.33	Fixed
α^1	Housing exp. share for type 1	0.20	Fixed
ψ^0	Pref. for leisure	0.25	Fixed
ψ^1	Pref. for leisure	0.25	Fixed
ν^0	Importance of Deterministic Utility for n	3.3	Fixed
ν^1	Importance of Deterministic Utility for n	3.3	Fixed
χ_1^0	Amenities in Zone 1	1.0	Normalized
χ_1^1	Amenities in Zone 1	1.0	Normalized
χ_2^0	Amenities in Zone 2	0.795	Calibrated
χ_2^1	Amenities in Zone 2	0.863	Calibrated

Notes: 1) Superscript 0 denotes low-skill household, superscript 1 denotes high-skill (college graduate) household.

Table 3: Model Prediction for Distribution of Incomes and Population

Row		Pre-COVID Baseline (1)	COVID Scenarios Start (2)	End (3)	Post-COVID Scenarios SR (4)	LR (5)	LR Putty-Clay (6)
	Technology:						
(1)	A^b	0.936	0.452	0.442	0.926	0.923	0.925
(2)	A^h	0.453	0.453	0.607	0.607	0.607	0.607
	Incomes:						
(3)	Type 1/0 Ratio of Labor Income	1.80	1.75	1.95	1.93	1.95	1.95
(4)	Type 0 Income per Worker	3.01	2.66	2.88	3.12	3.10	3.13
(5)	Living in Zone 1	3.08	2.73	2.95	3.19	3.17	3.21
(6)	Living in Zone 2	2.87	2.54	2.75	2.97	2.96	2.98
(7)	Type 1 Income per Worker	5.41	4.67	5.63	6.03	6.03	6.10
(8)	Living in Zone 1	5.47	4.59	5.50	6.01	5.98	6.06
(9)	Living in Zone 2	5.33	4.77	5.77	6.05	6.10	6.14
	Consumption:						
(10)	Type 1/0 Ratio of Consumption	1.73	1.54	1.66	1.79	1.78	1.80
	Population:						
(11)	Total Low Skill	67%	67%	67%	67%	67%	67%
(12)	Living in Zone 1	64%	66%	67%	65%	64%	64%
(13)	Living in Zone 2	36%	34%	33%	35%	36%	36%
(14)	Total High Skill	33%	33%	33%	33%	33%	33%
(15)	Living in Zone 1	59%	56%	55%	58%	56%	57%
(16)	Living in Zone 2	41%	44%	45%	42%	44%	43%

Notes: 1) We parameterize the model to the pre-COVID world. 2) In columns (2)-(4), we cut $\bar{A}^b$ by 50% to capture social distancing from the pandemic. 3) Columns (3)-(6) capture the improvement in work-from-home technology during the pandemic by increasing A^h to the level required to double the share of hours worked from home for type 1 in going from columns (1) to (4). 4) We hold the supply of space fixed at the pre-COVID baseline in counterfactuals (2)-(4). In counterfactual (5), we adjust the supply of space such that rents are equal to their pre-COVID benchmark in column (1). In column (6), we keep the stock of office space at the level in column (1) but adjust the stocks of residential space such that residential rents return to the level in column (1).

Table 4: Model Predictions for Work Location, Space, and Rents

Row		Pre-COVID	COVID Scenarios		Post-COVID Scenarios		
		Baseline	Start	End	SR	LR	LR Putty-Clay
		(1)	(2)	(3)	(4)	(5)	(6)
	Hours Worked:						
(17)	Type 0 Hours per Worker	0.69	0.69	0.69	0.69	0.69	0.69
(18)	Type 1 Effective Hours per Worker	0.74	0.52	0.65	0.82	0.81	0.83
(19)	Type 1 Hours Worked in CBD per Worker	0.57	0.25	0.13	0.44	0.40	0.43
(20)	Living in Zone 1	0.61	0.28	0.16	0.48	0.45	0.47
(21)	Living in Zone 2	0.51	0.20	0.10	0.38	0.34	0.36
(22)	Type 1 Hours Worked at Home per Worker	0.14	0.52	0.64	0.29	0.34	0.31
(23)	Living in Zone 1	0.12	0.48	0.62	0.26	0.30	0.27
(24)	Living in Zone 2	0.18	0.56	0.67	0.34	0.39	0.36
(25)	Ratio Hours Worked at Home to Total Hours	0.20	0.68	0.83	0.40	0.46	0.42
(26)	Living in Zone 1	0.16	0.63	0.80	0.35	0.40	0.36
(27)	Living in Zone 2	0.26	0.74	0.87	0.48	0.54	0.50
	Demand for Space:						
(28)	Aggregate Office Space in CBD	0.31	0.31	0.31	0.31	0.23	0.31
(29)	Aggregate Space in Zone 1	1.94	1.94	1.94	1.94	2.11	2.13
(30)	Home Office per Type 1	0.49	1.61	2.07	1.02	1.28	1.18
(31)	Per Type 1 Other Housing per Person	3.03	2.44	2.43	2.91	3.16	3.23
(32)	Per Type 0 Housing per Person	2.91	2.71	2.52	2.72	2.99	3.02
(33)	Aggregate Space in Zone 2	1.66	1.66	1.66	1.66	2.00	1.98
(34)	Home Office per Type 1	1.03	2.59	3.07	1.89	2.48	2.31
(35)	Per Type 1 Other Housing per Person	4.23	3.36	3.33	4.01	4.58	4.66
(36)	Per Type 0 Other Housing per Person	3.95	3.41	3.09	3.56	4.06	4.10
	Rent per Unit of Space:						
(37)	CBD	1.00	0.34	0.22	0.83	1.00	0.81
(38)	Zone 1	0.35	0.33	0.39	0.39	0.35	0.35
(39)	Zone 2	0.24	0.25	0.29	0.28	0.24	0.24

Notes: 1) See notes to Table 3.

Table 5: The Effect of Availability of Technology: A Hypothetical 1990 Pandemic

Row		Hypothetical 1990 Pandemic Pre-COVID (1)	Hypothetical 1990 Pandemic COVID Start (2)	2020 Pandemic Pre-COVID (3)	2020 Pandemic COVID Start (4)
	Technology:				
(1)	A^b	0.94	0.47	0.94	0.45
(2)	A^h	0.14	0.14	0.45	0.45
	Hours Worked:				
(3)	Type 0 Hours per Worker	0.69	0.69	0.69	0.69
(4)	Type 1 Effective Hours per Worker	0.71	0.36	0.74	0.52
(5)	Type 1 Hours Worked at Home per Worker	0.00	0.02	0.14	0.52
(6)	Ratio Hours Worked at Home to Total Hours	0.00	0.03	0.20	0.68
	Incomes:				
(7)	Type 0 Income per Worker	2.96	2.37	3.01	2.66
(8)	Type 1 Income per Worker	5.06	3.25	5.41	4.67
	Demand for Space:				
(9)	Aggregate Office Space in CBD	0.37	0.37	0.31	0.31
(10)	Aggregate Space in Zone 1	1.83	1.83	1.94	1.94
(11)	Aggregate Space in Zone 2	1.45	1.45	1.66	1.66
	Rent per Unit of Space:				
(12)	CBD	1.00	0.63	1.00	0.34
(13)	Zone 1	0.35	0.26	0.35	0.33
(14)	Zone 2	0.24	0.18	0.24	0.25

Table 6: Sensitivity of Results to EOS Between Work at Home and Office

		Pre-COVID	COVID Scenarios		Post-COVID Scenarios		
		Baseline	Start	End	SR	LR	LR Putty-Clay
Row		(1)	(2)	(3)	(4)	(5)	(6)
	A. Technology						
(1)	A^b	0.94	0.45	0.44	0.93	0.92	0.92
(2)	A^h	0.45	0.45	0.61	0.61	0.61	0.61
				EOS=3			
(3)	A^b	0.94	0.46	0.45	0.93	0.92	0.93
(4)	A^h	0.31	0.31	0.53	0.53	0.53	0.53
				EOS=7			
(5)	A^b	0.94	0.44	0.43	0.93	0.92	0.92
(6)	A^h	0.51	0.51	0.64	0.64	0.64	0.64
	B. Rents						
				EOS=5			
(7)	CBD	1.00	0.34	0.22	0.83	1.00	0.81
(8)	Zone 1	0.35	0.33	0.39	0.39	0.35	0.35
(9)	Zone 2	0.24	0.25	0.29	0.28	0.24	0.24
				EOS=3			
(10)	CBD	1.00	0.51	0.39	0.86	1.00	0.85
(11)	Zone 1	0.35	0.30	0.37	0.40	0.35	0.35
(12)	Zone 2	0.24	0.21	0.27	0.28	0.24	0.24
				EOS=7			
(13)	CBD	1.00	0.23	0.14	0.81	1.00	0.79
(14)	Zone 1	0.35	0.35	0.40	0.38	0.35	0.35
(15)	Zone 2	0.24	0.27	0.30	0.27	0.24	0.24
	C. Incomes						
				EOS=5			
(16)	Type 1 / 0 Income	1.80	1.75	1.95	1.93	1.95	1.95
(17)	Type 1 Income / Worker	5.41	4.67	5.63	6.03	6.03	6.10
(18)	Type 0 Income / Worker	3.01	2.66	2.88	3.12	3.10	3.13
				EOS=3			
(19)	Type 1 / 0 Income	1.80	1.62	1.88	1.98	1.98	1.99
(20)	Type 1 Income / Worker	5.41	4.18	5.39	6.30	6.29	6.37
(21)	Type 0 Income / Worker	3.01	2.58	2.86	3.19	3.18	3.20
				EOS=7			
(22)	Type 1 / 0 Income	1.80	1.84	2.00	1.92	1.95	1.94
(23)	Type 1 Income / Worker	5.41	5.01	5.81	5.94	5.97	6.02
(24)	Type 0 Income / Worker	3.01	2.73	2.91	3.09	3.07	3.10

Table 7: Greater Agglomeration Economies in the CBD

		Pre-COVID	COVID Scenarios		Post-COVID Scenarios		
		Baseline	Start	End	SR	LR	LR Putty-Clay
Row		(1)	(2)	(3)	(4)	(5)	(6)
	A. Technology						
		$\delta_b = 0.04$ (benchmark)					
(1)	A^b	0.94	0.45	0.44	0.93	0.92	0.92
(2)	A^h	0.45	0.45	0.61	0.61	0.61	0.61
		$\delta_b = 0.10$					
(3)	A^b	0.85	0.39	0.36	0.83	0.82	0.82
(4)	A^h	0.41	0.41	0.54	0.54	0.54	0.54
	B. Rents						
		$\delta_b = 0.04$					
(5)	CBD	1.00	0.34	0.22	0.83	1.00	0.81
(6)	Zone 1	0.35	0.33	0.39	0.39	0.35	0.35
(7)	Zone 2	0.24	0.25	0.29	0.28	0.24	0.24
		$\delta_b = 0.10$					
(8)	CBD	1.00	0.30	0.18	0.82	1.00	0.80
(9)	Zone 1	0.35	0.33	0.38	0.38	0.35	0.35
(10)	Zone 2	0.24	0.25	0.29	0.27	0.24	0.24
	C. Incomes						
		$\delta_b = 0.04$					
(11)	Type 1 / 0 Income	1.80	1.75	1.95	1.93	1.95	1.95
(12)	Type 1 Income / Worker	5.41	4.67	5.63	6.03	6.03	6.10
(13)	Type 0 Income / Worker	3.01	2.66	2.88	3.12	3.10	3.13
		$\delta_b = 0.10$					
(14)	Type 1 / 0 Income	1.80	1.76	1.95	1.92	1.94	1.94
(15)	Type 1 Income / Worker	5.41	4.66	5.56	5.97	5.95	6.02
(16)	Type 0 Income / Worker	3.01	2.65	2.85	3.10	3.07	3.11

Figure 1: Share of EU15 Workers Working from Home, 1995-2019

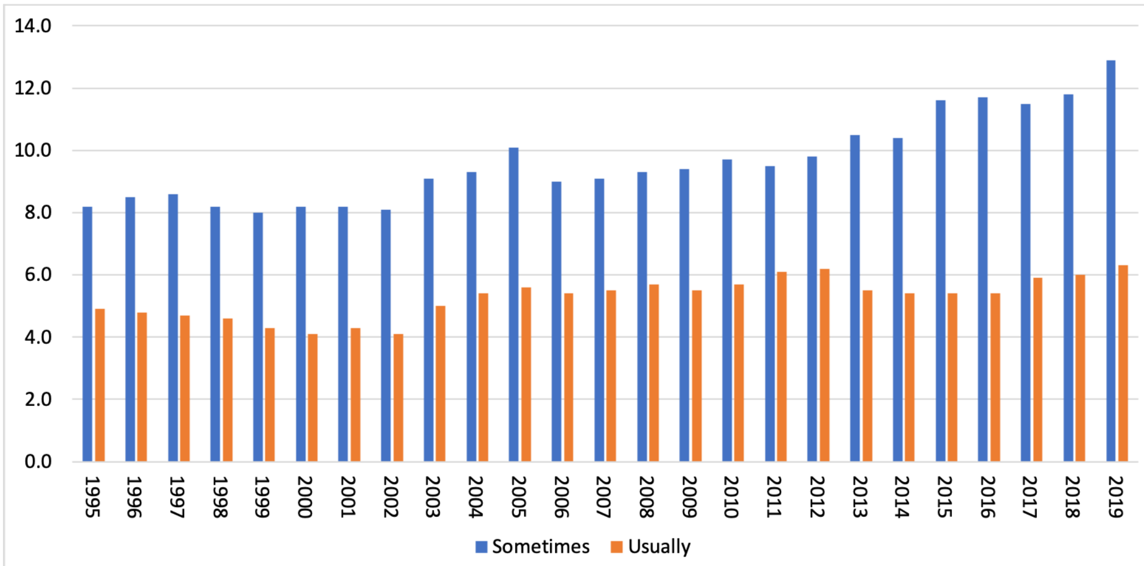

Notes: 1) Includes all employed workers aged 25-64. 2) Source: Eurostat and authors' calculations.

Figure 2: The Sensitivity of Work-at-Home to Changes in Productivity

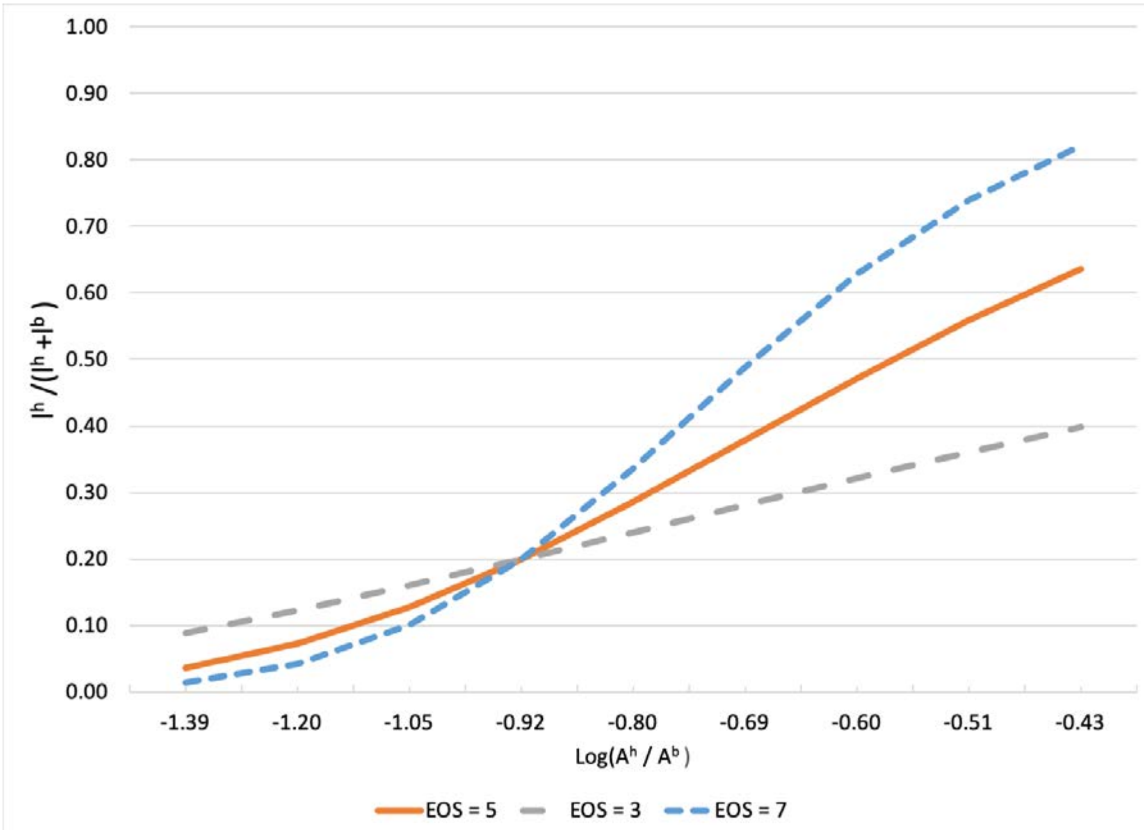

Notes: 1) The figure plots the share of work done at home for high-skill workers (y-axis) against log of relative TFP of work at home $\log\left(A^h/A^b\right)$ for three different values of the EOS. The solid line represents our benchmark parameterization of the EOS.

A Using Commute Times to Estimate the EOS between Work at Home and the Office

A.1 The Linear Approximation of the Logistic Function

Define the logistic function in x as

$$f(x) \;=\; \frac{e^{a+bx}}{1 \;+\; e^{a+bx}}$$

A first order approximation to $f(x)$ around $\bar{x}$ is

$$\begin{aligned} f(x) &\approx f(\bar{x}) + f'(\bar{x})(x-\bar{x}) \\ &= f(\bar{x}) + f(\bar{x})\left[1-f(\bar{x})\right]b(x-\bar{x}) \\ &= \widetilde{a} \quad\; + f(\bar{x})\left[1-f(\bar{x})\right]bx \end{aligned} \tag{A.1}$$

where $\widetilde{a} \;=\; f(\bar{x})\left\{1 \;-\; \left[1-f(\bar{x})\right]b\bar{x}\right\}$.

In Table 1, we estimate the parameters of $f(x)$ for $x = \ln(1+t)$ using GMM and observed data on the fraction of days individuals work at home. We can thus map the approximation in Equation (A.1) to our strategy for estimating Ψ. We set $b = -3.0$ which is approximately equal to the estimate of Ψ in columns 1 and 2 of Table 1, $\bar{x} = 0.10$ (its sample average), and $a = 2.5$ which yields $f(\bar{x}) = 0.9$, roughly the sample average of $f(x)$ in our data.

Figure A.1 graphs $f(x)$ and its linear approximation for this parameterization. The figure shows $f(x)$ and its approximation for all commutes in the data; the vertical red lines bracket the middle 95% of commutes. The figure shows that for all commutes, but especially the 95% of commutes between the vertical lines, the linear approximation yields very close values to the actual function.

In the event that x is not measured with error, the near linearity of $f(x)$ for actual commute times and fraction of days worked shown in Figure A.1 suggests that if we were to run a linear regression of y on x, the regression coefficient would be approximately equal to

$$\widehat{\gamma}^{OLS} \approx bf(\bar{x})\left[1 - f(\bar{x})\right]. \tag{A.2}$$

This near linearity also implies that an unbiased estimate of b from GMM, $\widehat{b}^{GMM}$, has the property

$$\widehat{b}^{GMM} \approx \frac{\widehat{\gamma}^{OLS}}{f(\bar{x})\left[1 - f(\bar{x})\right]}. \tag{A.3}$$

We believe that x is measured with error, such that when y is regressed on measured x, the regression coefficient from OLS will be equal to the estimate in equation (A.2) times ζ, where ζ is the attenuation bias due to the presence of measurement error. In the next section, we derive ζ^{-1}, the exact correction for attenuation bias in the case of OLS. Equations (A.2) and (A.3) suggest this correction will also work for our GMM estimate. The next section verifies this conjecture using a Monte Carlo simulation.

A.2 Monte Carlo Simulation of Analytical Bias Correction

A.2.1 Commute Time Data Generating Process

We conduct Monte Carlo simulation experiments to assess the performance of our proposed bias correction. The data generating process that we consider is,

$$\begin{aligned} i &= 1, ..., N \\ x_i^* &\sim N(\mu_{x^*}, \sigma^2_{x^*}) \end{aligned}$$

$$\begin{aligned} y_{it} &= \begin{cases} 1 \text{ with probability } & = \Lambda(a + bx_i^*) \\ 0 \text{ with probability } & = 1 - \Lambda(a + bx_i^*) \end{cases} \text{, for } t = 1, ..., T \\ \overline{y}_i &= \frac{1}{T}\sum_{t=1}^{T} y_{it} \end{aligned}$$

There are N individuals. Each individual draws x_i^* from a normal distribution. The variable has a causal effect (logit parameter b) on the probability that a binary outcome y equals one. Each individual realizes $T = 5$ Bernoulli draws y_{it}, the average of which is $\overline{y}_{it}$.

The econometrician does not observe x_i^*, but does observe two measures

$$\begin{aligned} x_{i1} &= x_i^* + e_1 \\ x_{i2} &= x_i^* + e_2 \end{aligned}$$

$$\begin{bmatrix} e_{i1} \\ e_{i2} \end{bmatrix} \sim N\left(\begin{bmatrix} 0 \\ 0 \end{bmatrix}, \begin{bmatrix} \sigma_e^2 & \rho_e\sigma_e^2 \\ \rho_e\sigma_e^2 & \sigma_e^2 \end{bmatrix}\right)$$

The measurement errors e_{i1} and e_{i2} are uncorrelated with x_i^* but are potentially correlated with one another (correlation ρ_e).

Our experiments involve simulating $R = 1,000$ datasets from this process for each of value of $\rho_e = 0, .1, .2, .3, .4, .5$. In each dataset, we compute the naive (ignoring measurement error) logit GMM estimator $\widehat{b}^{GMM}$ using the mis-measured variable x_1 as the only right-hand side regressor, and our proposed bias-corrected estimator $\widehat{b}^{BC}$. The naive GMM estimator solves,

$$(\widehat{a}^{GMM}, \widehat{b}^{GMM}) = \arg\min_{(a,b)} \widehat{m}'(a,b)\, \mathcal{W}\, \widehat{m}(a,b)$$

where

$$\begin{aligned}
\epsilon_i(a,b) &= \overline{y}_i - \Lambda(a + b x_{i1}) \\
\widehat{m}_0(a,b) &= \sum_i \epsilon_i(a,b) \\
\widehat{m}_1(a,b) &= \sum_i x_{i1}\epsilon_i(a,b) \\
\widehat{m}(a,b) &= \begin{bmatrix} \widehat{m}_0(a,b) \\ \widehat{m}_1(a,b) \end{bmatrix}
\end{aligned}$$

and $\mathcal{W}$ is an optimal weighting matrix. As described in the text, the bias-corrected estimator is computed using

$$\begin{aligned}
\widehat{b}^{BC} &= \widehat{b}^{GMM} \left(\frac{\widehat{var}(x_1)}{\widehat{var}(x^*)} \right) \\
&= \widehat{b}^{GMM} \left(\frac{\widehat{var}(x_1)}{\widehat{var}(x_1) - \widehat{var}(e)} \right) \\
&= \widehat{b}^{GMM} \left(\frac{\widehat{var}(x_1)}{\widehat{var}(x_1) - \left(\frac{\widehat{var}(x_1) - \widehat{cov}(x_1, x_2)}{1 - \rho_e} \right)} \right) \qquad \text{(A.4)}
\end{aligned}$$

where ρ_e is an assumed value, and $\widehat{var}(x_1)$, $\widehat{cov}(x_1, x_2)$ are computed in the (simulated) data.

A.2.2 Parameter Values for Simulations

For each simulated dataset, we set $N = 1700$. We do separate experiments for each value of ρ_e $\rho_e = 0, .1, .2.3, .4$ and $.5$. At each assumed ρ_e, we choose values for the other parameters of the data generating process to match three moments from the actual commute data.

- Data moment var$(\ln(1 + t_{i1})) = .0707^2 = .005$ to set $var(x_1) = .005$
- Data moment cov$\big(\ln(1 + t_{i1}), \ln(1 + t_{i2})\big) = .00348$ to set $cov(x_1, x_2) = .00348$
- Naive estimator $\widehat{\Psi}^{GMM} \approx -3$ to set b (by targeting the attenuated $\widehat{b}^{GMM}$)

To find the values of $\sigma^2_{x^*}$ and σ^2_e that are consistent with these moments, we note that

$$
\begin{aligned}
var(x_1) &= \sigma^2_{x^*} + \sigma^2_e \\
cov(x_1, x_2) &= \sigma^2_{x^*} + \rho_e \sigma^2_e
\end{aligned}
$$

which imply

$$
\begin{aligned}
\sigma^2_e &= \frac{var(x_1) - cov\big(x_1, x_2\big)}{1 - \rho_e} = \frac{.005 - .00348}{1 - \rho_e} \\
\sigma^2_{x^*} &= var(x_1) - \sigma^2_e = .005 - \sigma^2_e
\end{aligned}
$$

Beginning with equation (A.4), we set

$$
\begin{aligned}
b &= \widehat{b}^{GMM} \times \left(\frac{var(x_1)}{var(x_1) - \left(\frac{var(x_1) - cov(x_1, x_2)}{1 - \rho_e} \right)} \right) \\
&= -3 \times \left(\frac{.005}{.005 - \left(\frac{.005 - .00348}{1 - \rho_e} \right)} \right)
\end{aligned}
$$

We choose $\mu_{x^*} = 0.1$ and thus set $a = 1.7$ to approximately match the unconditional fraction of days spent working in the office.

A.2.3 Results

In each simulated dataset, we compute the naive GMM estimator $\widehat{b}^{GMM}$ and compute the corresponding bias corrected estimator using equation (A.4). Table A.1 summarizing the results. For each value of ρ_e, the bias corrected estimator has a sampling mean that is close to the assumed value of b, which occurs because the naive GMM estimator has a sampling mean that is close to -3, suggesting that, under a correct assumptions of ρ_e, the bias-corrected GMM estimator provides unbiased estimates of b with measurement error in x_1 and x_2 that mimics the properties of the measurement error in our commute data.

Table A.1: Monte Carlo Simulation Results

ρ_e	Assumed b	$\widehat{b}^{BC}$	$\widehat{b}^{GMM}$
0.0	-4.31	-4.30	-2.99
0.1	-4.53	-4.51	-2.98
0.2	-4.84	-4.85	-3.00
0.3	-5.30	-5.26	-2.98
0.4	-6.08	-6.05	-2.98
0.5	-7.65	-7.56	-2.96

Figure A.1: Logistic Function and First-Order Approximation

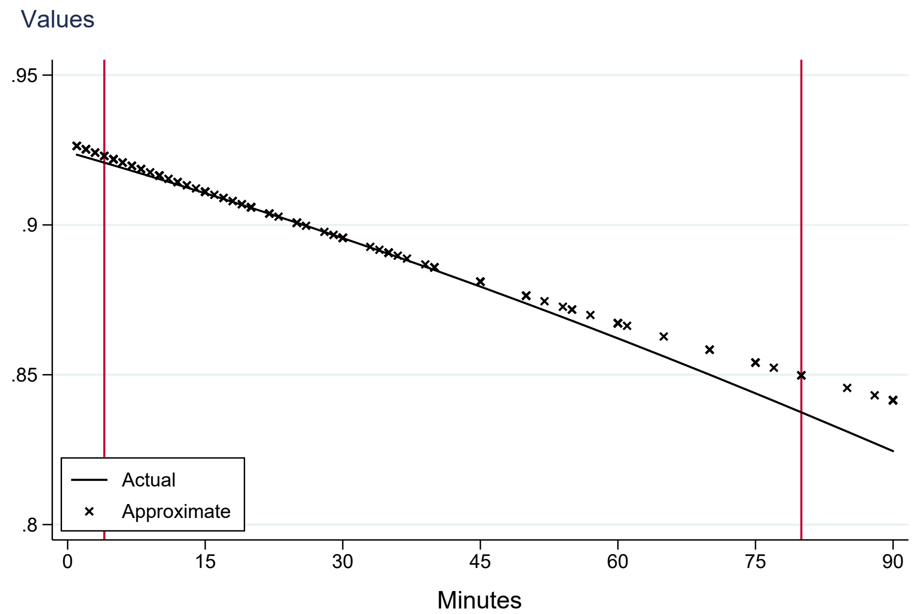

Notes: 1) Recall that $t = 2 * \text{minutes}/\,(8 * 60)$, where minutes refers to the time required for a one-way commute to work.

Figure A.2: Differences in and Levels of Reported Commute Times

(a) Absolute Value of Difference of Individual Reported Commutes

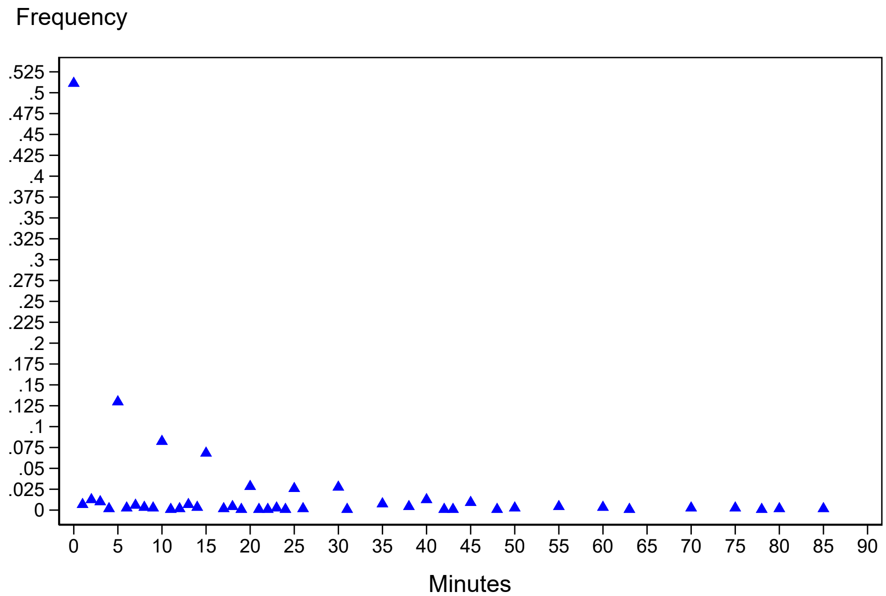

(b) Raw Distribution of Individual Reported Commutes